*Article*

# Characterization of Carbon Nanomaterials Dispersions: Can Metal Decoration of MWCNTs Improve Their Physicochemical Properties?

Ana T. S. C. Brandão [1], Sabrina Rosoiu [2], Renata Costa [1], A. Fernando Silva [1], Liana Anicai [2,3], Marius Enachescu [2,4] and Carlos M. Pereira [1,*]

1   CIQUP—Physical Analytical Chemistry and Electrochemistry Group, Departamento de Química e Bioquimica, Faculdade de Ciências da Universidade do Porto, Rua do Campo Alegre, 687, 4169007 Porto, Portugal; up200706627@edu.fc.up.pt (A.T.S.C.B.); renata.costa@fc.up.pt (R.C.); afssilva@fc.up.pt (A.F.S.)
2   Center for Surface Science and Nanotechnology, University Polytechnica of Bucharest, Splaiul Independentei, 313, 060042 Bucharest, Romania; sabrina.rosoiu@cssnt-upb.ro (S.R.); liana.anicai@cssnt-upb.ro (L.A.); marius.enachescu@cssnt-upb.ro (M.E.)
3   OLV Development SRL, Brasoveni 3, 023613 Bucharest, Romania
4   Academy of Romanian Scientists, Splaiul Independentei 54, 050094 Bucharest, Romania
*   Correspondence: cmpereir@fc.up.pt

**Abstract:** A suitable dispersion of carbon materials (e.g., carbon nanotubes (CNTs)) in an appropriate dispersant media, is a prerequisite for many technological applications (e.g., additive purposes, functionalization, mechanical reinforced materials for electrolytes and electrodes for energy storage applications, etc.). Deep eutectic solvents (DES) have been considered as a promising "green" alternative, providing a versatile replacement to volatile organic solvents due to their unique physical-chemical properties, being recognized as low-volatility fluids with great dispersant ability. The present work aims to contribute to appraise the effect of the presence of MWCNTs and Ag-functionalized MWCNTs on the physicochemical properties (viscosity, density, conductivity, surface tension and refractive index) of glyceline (choline chloride and glycerol, 1:2), a Type III DES. To benefit from possible synergetic effects, AgMWCNTs were prepared through pulse reverse electrodeposition of Ag nanoparticles into MWCNTs. Pristine MWCNTs were used as reference material and water as reference dispersant media for comparison purposes. The effect of temperature (20 to 60 °C) and concentration on the physicochemical properties of the carbon dispersions (0.2–1.0 mg cm$^{-3}$) were assessed. In all assessed physicochemical properties, AgMWCNTs outperformed pristine MWCNTs dispersions. A paradoxical effect was found in the viscosity trend in glyceline media, in which a marked decrease in the viscosity was found for the MWCNTs and AgMWCNTs materials at lower temperatures. All physicochemical parameters were statistically analyzed using a two-way analysis of variance (ANOVA), at a 5% level of significance.

**Keywords:** deep eutectic solvent; carbon nanotube; silver nanoparticles; viscosity; ionic conductivity; surface tension; activation energy

## 1. Introduction

Carbon nanotubes (CNTs) were first reported by Iijima [1], receiving much interest due to their properties such as high aspect ratio, lightweight, high tensile strength, excellent electrical conductivity and stability [2–4]. The outer layer of the CNTs can be used as an anchor for the deposition of metallic nanoparticles (NPs) [3]. NPs incorporation is of great interest because they can form hybrid nanostructures that exhibit enhanced [5] or novel properties, due to size, large surface area and quantum dimension, which can enhance their physical and chemical properties [6]. Several metals (e.g., Ag, Au, and Pt) have been explored for the decoration of CNTs [7–10]. However, Ag nanoparticles (Ag-NPs) have

received unique attention [11–18] due to their high conductivity, which contributes to the improvement of the electrical conductivity of the CNTs composites.

The electrolyte reaction media considered to entrap metallic NPs into the carbon matrix have also captured great attention due to their high impact on the chemical properties, mechanical stability and compatibility with enhanced surface area and electrical properties [19]. Non-aqueous solvents may present some advantages compared to aqueous solvents [19–21], when the dispersibility and the electrochemical stability is taken into consideration [22]. Ionic liquids (ILs) present high production and purification costs, making these dense non-aqueous fluids less competitive when compared with traditional solvents.

Alternatively, deep eutectic solvents (DES) have emerged as suitable and attractive "green" alternatives to ILs for many chemical processes and are often described as ILs analogues in the literature [20]. Due to their unique compositional flexibility, intermolecular interactions and physicochemical properties, DES are pointed as a good dispersion media for carbon materials, such as CNTs [21].

Cojocaru et al. [18] suggested for the first time, the electrochemical synthesis of Ag-NPs involving choline chloride-glycerol based DES using pulse reversed current technique using a two-electrode cell, in which the $Ag^+$ ions are produced by anodic dissolution of the Ag metal or dissolution of the Ag-based salt. Poly(*N*-vinyl pyrrolidone) (PVP) was used as a capping agent to avoid agglomeration and to control the growth of the Ag NPs [23]. Following the works by Brandão et al. [24] and Cojocaru et al. [18], the electrochemical decoration of MWCNTs with Ag-NPs from choline chloride–glycerol eutectic mixture, using pulse reversed current in a two-electrode cell can be successfully achieved. Water-glyceline based DES binary systems have been successfully used in assisting and optimizing the dispersion efficiency of carbon nanotubes in water, allowing to predict the fate and transport of SWCNTs in aqueous DES systems [21].

Several studies have been carried out regarding the thermophysical properties of several ILs and DES [25–33], and both have been proved to be good dispersant media for CNTs dispersion [21,34–39].

CNTs dispersions can be used for many applications, such as lubricants [40–42], polymer nanocomposites [43], and more recently it has been drawing the attention of the scientific community for the development of next-generation porous solid-state electrolytes [44–47] and as electrode materials [48].

To the best of our knowledge, it is the first time that properties such as viscosity, density, conductivity, refractive index, and surface tension of MWCNTs and AgMWCNTs/DES-nanomaterial dispersions in glyceline have been gathered and further compared with water dispersions of the same materials. Further, several methods of AgMWCNTs/DES-nanomaterial synthesis were studied to infer the effect of synthesis parameters on the performance of AgMWCNTs dispersions in DES.

The synthesis of AgMWCNTs in DES is expected to achieve a double goal, as it is predicted to improve the surface wettability of the composite material by the solvent but also to markedly increase the capacitance of interfaces between composite electrodes, containing the metallic nanoparticles decorated carbon nanotubes, and DES [24]. The dispersion of MWCNTs and AgMWCNTs in DES may present a valuable route to obtain dispersions with enhanced properties for application in advanced energy storage devices.

## 2. Materials and Methods

### 2.1. Preparation of DES

Choline chloride (Sigma Aldrich, 99%, Darmstadt, Germany) was dried overnight in the oven, at 60 °C, before use; glycerol (Sigma Aldrich, 99%, Darmstadt, Germany), and poly (N-vinyl pyrrolidone) (PVP 10, Sigma Aldrich, Darmstadt, Germany) were used as received. The eutectic mixture (known as glyceline) was formulated by mixing and heating at 60 °C the ChCl with glycerol, as HBD, in the molar ratio of 1:2, until a homogeneous and clear liquid was formed.

Before the physicochemical studies, glyceline water content (wt.%) was determined using a Karl Fischer titrator (831 KF Coulometer, Methrom (Herisau, Switzerland)). The sample solution was manually mixed to achieve the maximum homogenization before titrating. A 1 cm$^3$ of a sample (~1.15 g) was added to the dry methanol solvent (HY-DRANAL™, max 0.01 wt.% water, Riedel−de−Haën (Honeywell Specialty Chemicals Seelze GmbH Charlotte, USA)) and titrated with HYDRANAL™ Composite 5 Reagent (4.5–5.5 mg mL$^{-1}$ water equivalent, Riedel−de−Haën (Honeywell Specialty Chemicals Seelze GmbH Charlotte, USA)) for moisture determination. Measurements were performed in triplicate and the water content in glyceline was found to be 6.3 ± 0.5 wt.%.

Commercial MWCNTs (Sigma Aldrich, 99%, Darmstadt, Germany) were dispersed in the glyceline media, followed by ultrasonication for 4 h. The MWCNTs have an average diameter of 24 ± 4 nm, determined by Scanning electron microscopy image analysis (SEM, Hitachi SU 8230 equipment (Krefeld, Germany)).

## 2.2. Electrochemical Synthesis of Ag Nanoparticles and Decoration of MWCNTs

The electrochemical synthesis of Ag-NPs on the surface of MWCNTs was previously described by Brandão et al. [24]. Briefly, AgMWCNTs/DES were synthesized by a pulse reverse current mode (pe 86CB 3HE, plating electronic GmbH), at room temperature, using a two-electrode cell configuration with 50 mL of glyceline. Both electrodes were composed of Ag wires with an exposed area of approximately 5 cm$^2$. Before each synthesis, the Ag wires were hand polished and washed with distilled water, and dried.

Different applied anodic and cathodic currents, and different on ($t_{ON}$) and off-times ($t_{OFF}$) were used to prepare the Samples A to E, details of which are presented in Table S1, in Supplementary Materials. All electrodepositions were performed under magnetic stirring or ultrasonication. To recover the AgMWCNT, the electrolyte was centrifuged at 4000 rpm for 20 min, with intermediary washing with ethanol and hot water to remove the eutectic mixture. After AgMWCNT separation, the material was dried overnight at 60 °C and used without any further treatment. The main characteristics (amount, size, and specific capacitance) of the materials A to E are listed in Table 1.

**Table 1.** Characteristics of the Ag NPs, particularly Ag NPs content, size, and specific capacitance of the different samples. Data from Brandão et al. [24] *.

| Samples | Ag NPs Amount/wt. % (from EDX Analysis) | Ag NPs Size/nm (from SEM Image) | Specific Capacitance /F g$^{-1}$ (using 3 Electrode Cell) |
|---|---|---|---|
| A | 3 ± 1 | 12 ± 5 | 5.2 ± 0.3 |
| B | 11 ± 3 | 16 ± 4 | 14.6 ± 1.0 |
| C | 1.0 ± 0.2 | 18 ± 3 | 7.1 ± 0.8 |
| D | 28 ± 8 | 33 ± 6 | 16.3 ± 1.2 |
| E | 24 ± 9 | 46 ± 7 | 28.5 ± 1.6 |

* Reprinted from Characterization and electrochemical studies of MWCNTs decorated with Ag nanoparticles through pulse reversed current electrodeposition using a deep eutectic solvent for energy storage applications, Pages No. 342–359, Copyright (2021), with permission from Elsevier.

## 2.3. Zeta Potential Analysis

The zeta potential (ZP) of particles was determined by electrophoretic mobility using the Helmholtz–Smoluchowski equation [49] through Zetasizer Nano ZS (Malvern Instruments, Malvern, UK). The values reported are the mean ± standard deviation of three different measurements recorded for each sample.

ZP was not calculated for the carbon-glyceline dispersions, due to the incapability of the equipment to measure these samples.

## 2.4. Physicochemical Characterization

### 2.4.1. Density and Dynamic Viscosity

Dynamic viscosities (η) and densities (ρ) of MWCNTs and AgMWCNTs dispersed in glyceline, and water were measured using the automated Anton Paar DMA™ 4500 M

micro viscometer (Anton Paar GmbH, Graz, Austria). The density measurement is based on electromagnetically induced oscillations of a U-shaped glass tube. The standard deviations associated with the density measurement were below 0.00005 g cm$^{-3}$. The viscosities were measured based on Hoeppler's falling ball principle. A 100 mm long capillary with a diameter of 3.0 mm (glyceline) or 1.6 mm (water) with a tilting angle from 24° to 70°. The standard deviation in dynamic viscosities data was below 0.5%.

All the physicochemical characterization measurements were performed in the temperature range between 20 °C and 60 °C, with 10 °C steps.

### 2.4.2. Refractive Index

Refractive index (RI) of both MWCNTs and AgMWCNTs dispersions in glyceline and water were determined using an Abbe Refractometer DR-A1-Plus (Atago Co, Ltd., Tokyo, Japan) with a resolution of ±0.00001 and uncertainty in the experimental measurements of ±0.0002. The apparatus was calibrated by measuring the refractive index of ultrapure water before the measurements, taking into consideration the values of RI vs. temperature of water already published [50].

### 2.4.3. Surface Tension

The measurement of the surface tension was performed in a homemade analyzer with temperature control, which is composed of a camera (Guppy F-036, Allied-vision, Stadtroda, Germany), and a sample holder. The measurement procedure was calibrated through the measurement of several drops of ultra-pure water at different temperatures. For every dispersion, 5 drops were formed to obtain an average and standard deviation. Once the drop is placed, an image is taken. The image is digitally processed and analyzed using the ImageJ software (W. Rasband, National Institutes of Health, Bethesda, MD, USA) with the Pendent Drop plug-in (Adrian Daerr, Paris, France) [51].

### 2.4.4. Ionic Conductivity

The ionic conductivity of the MWCNTs dispersions in glyceline and water was measured with Mettler Toledo Conductivity meter F30 (Columbus, OH, USA). An aqueous solution of KCl was used as a calibration standard. The temperature was stabilized with a thermostat for both calibration and experimental measurement.

### 2.5. Statistical Analysis

Statistical analysis (GraphPad Prism 9 software (Graphpad Holdings, San Diego, CA, USA) was employed to perform a two-way analysis of variance (ANOVA) of the experimental data at a 5% level of significance. Linear regression was performed to establish the correlation of every determined parameter with the evolution of temperature and concentration. All determinations were performed in triplicate and a relevant average value and standard deviation are reported.

## 3. Results and Discussion

### 3.1. Morphological Characterization

The morphological characterization of MWCNTs and Ag-MWCNTs composite samples prepared in this work was performed through SEM analysis, and the images are presented in Figure 1.

The SEM analysis for Samples A to E are displayed in Figure 1, showing the morphology of the Ag-MWCNTs composites with different electrodeposition parameters as detailed in Table 1. SEM analysis of AgMWCNTs (A–E) shows that Ag-NPs are located on the edges and surface of the MWCNTs, and presents some agglomerates of Ag-NPs (more evident in Samples D and E). The average diameter of the Ag-NPs is presented in Table 1. Sample E presents the higher amount of Ag, bigger size of Ag-NPs, and higher specific capacitance as previously published by Brandão et al. [24].
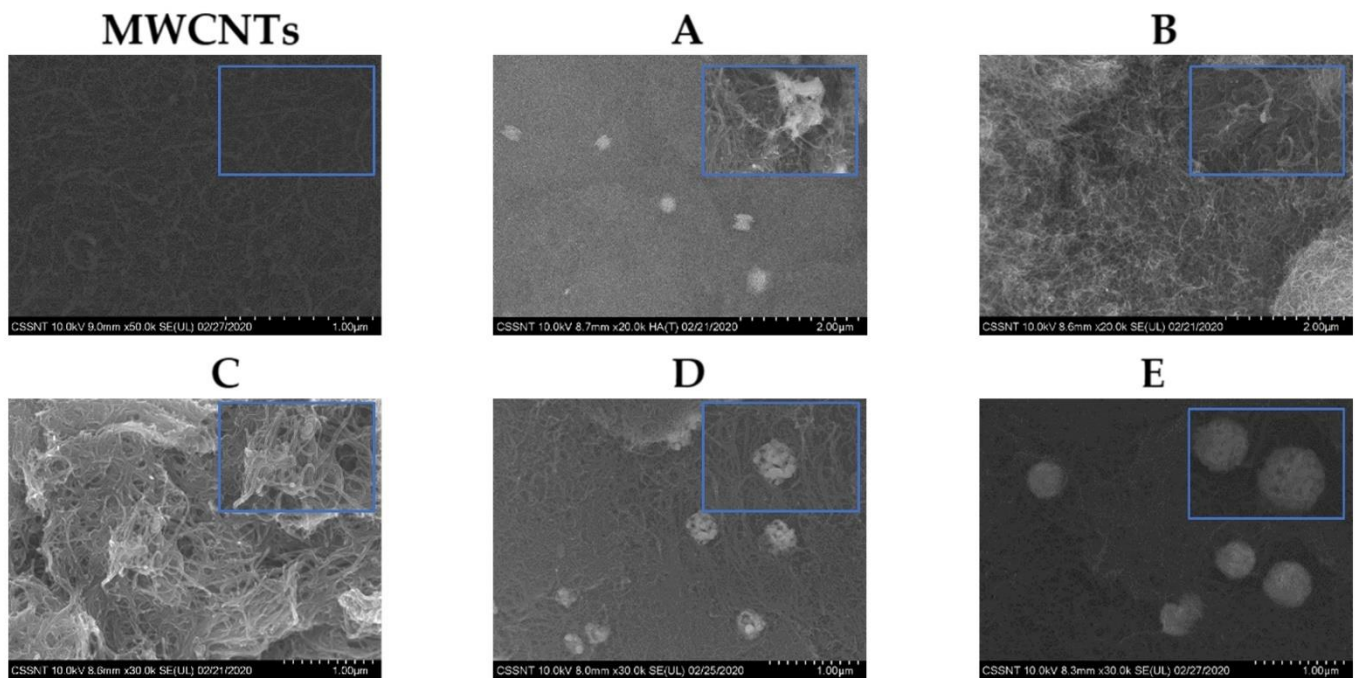
**Figure 1.** Electron microscopy images showing the structure of MWCNTs and AgMWCNTs samples (**A**–**E**) at different magnifications (20× and 100× (inset)).

### 3.2. Zeta Potential Analysis

The ZP analysis was performed for MWCNTs and AgMWCNTs samples dispersed in water, and the results are presented in Figure 2. The ZP obtained for the MWCNTs and the different AgMWCNTs samples, using a 0.4 mg cm$^{-3}$ dispersion (Figure 2a) shows that introducing the AgMWCNTs leads to the increase, towards more negative potentials, of ZP. This seems to be strictly associated to the presence of AgNPs, in particular with the increase of Ag NPs size. According to Sabri et al. [52], a high ZP value correlates to stable dispersion and the dispersed MWCNTs are well distributed. While the low ZP derives an attractive force that exceeds the repulsive force, the dispersion of the MWCNTs tends to aggregate. This is in line with the obtained results (Figure 2b,c), where an increase in the concentration of carbon materials in the water dispersions, leads to a decrease in the ZP values.
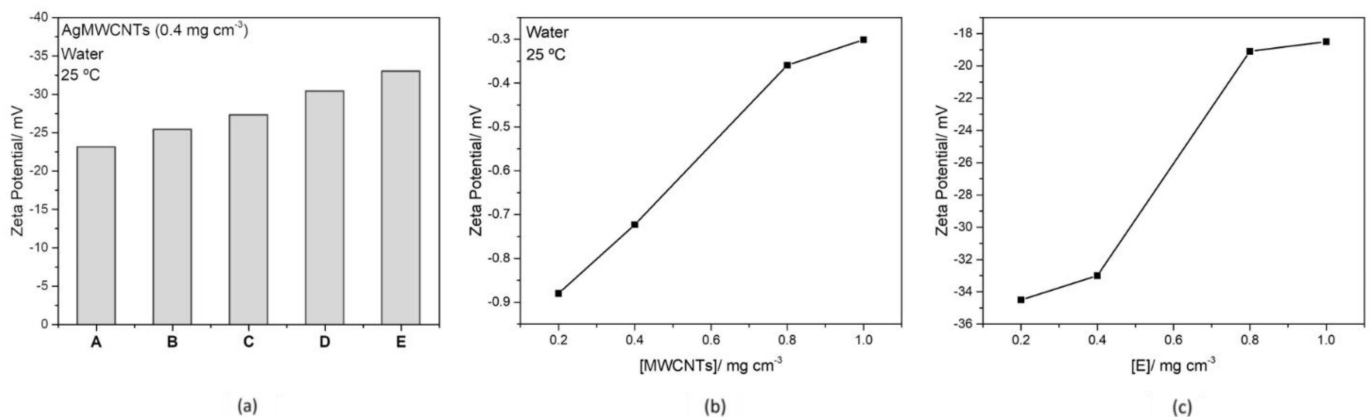


**Figure 2.** Zeta potential (ZP) for different AgMWCNTs samples (0.4 mg cm$^{-3}$) (**a**), different MWCNTs concentrations (**b**) and different concentrations of Sample E (**c**).

Figure 2a indicates that the dispersion of Sample E, with a bigger size of Ag NPs, presents a higher value of ZP, and consequently a more stable dispersion. Taking into

consideration the overall results, the decoration of MWCNT with Ag nanoparticles significantly changed the zeta potential (from $\approx -1$ mV to $-33$ mV AgMWCNT, Sample E). This change in zeta potential for modified MWCNTs is in agreement with other published work [53] and is compatible with increased stability of AgMWCNTs dispersions in water, making it suitable for the characterization of the physicochemical properties.

*3.3. Physicochemical Properties of MWCNTs and AgMWCNTs*

The physicochemical properties of MWCNTs and AgMWCNTs dispersions in glyceline, and water were measured and will be thoroughly discussed in this section. A detailed comparison will be presented for AgMWCNTs Samples A through E since they cover different features of the prepared AgMWCNTs, namely the effect of mass transport on the synthesis step (comparison between Samples B and E); the effect of the amount of Ag and size of Ag-NPs (comparison between Samples C and D, B and E and B and C). The detailed information regarding the parameters for the electrodeposition process of AgMWCNTs can be found in the Supplementary Materials (Table S1).

The detailed information regarding the physicochemical parameters of MWCNTs and AgMWCNTs dispersions can be found in Supplementary Materials, and it will be referred throughout the text as necessary.

3.3.1. Density

Solvent densities (ultrapure water and glyceline) were measured to allow the validation of the experimental procedure and to build a set of reference points to help understand the changes observed.

The measured density values for MWCNTs dispersed in glyceline and water, as a function of temperature is presented in Figure 3a,b respectively. The temperature dependence in glyceline (Figure 3a) is linear, however, in water (Figure 3b), it presents a slight curve. The linear decrease that can be seen in DES is due to the formation of larger intermolecular voids at higher temperatures, which increase the volume and decrease the density [54]. This effect was already described by several authors [54–57].

The density values for the different dispersions both in glyceline and water present similar results; however, in both cases, the introduction of the MWCNTs increases the density. The effect of MWCNTs is less pronounced in water, which, as expected, also presents a lower density compared to glyceline. Density values for pure glyceline found in the literature are listed in Table 2 and have a large range of values (namely the values found for 25 °C and 90 °C) and only a reduced number of works (e.g., the work of Crespo et. al. [27] and the present work) display the water content of the eutectic mixture. The value determined in the present work is in good agreement with the value reported by Crespo et. al. [27]. The density of ultrapure water is also in good agreement (less than 0.01% difference) with published values [58].

The decrease in density as a function of temperature is expected since an increase in temperature increases the DES molecules mobility and due to that, the thermal expansion of the DES volume increases [54]. The most important feature of the temperature effect in density is the fact that glyceline and their dispersions have a linear relationship with temperature.

The effect of Ag-NPs attached to the MWCNTs surface, dispersed in glyceline and water media is presented in Figure 3c (Samples B, D and E) and 3d (Samples A and C). To facilitate data interpretation Figure 3c,d present the ratio of $\rho_{\text{Ag-M WCNTs}}/\rho_{\text{MWCNTs}}$ as a function of temperature for samples at a fixed concentration (0.4 mg cm$^{-3}$), a similar effect is observed for all the other concentrations measured under this study. The measured density values of MWCNTs and AgMWCNTs mixtures (Samples A to E) as a function of temperature in the range 20 °C to 60 °C are presented in Supplementary Materials, in Figure S1a–f and Tables S2 and S3 and Figure S2a–f and Tables S4 and S5, respectively for glyceline and water.
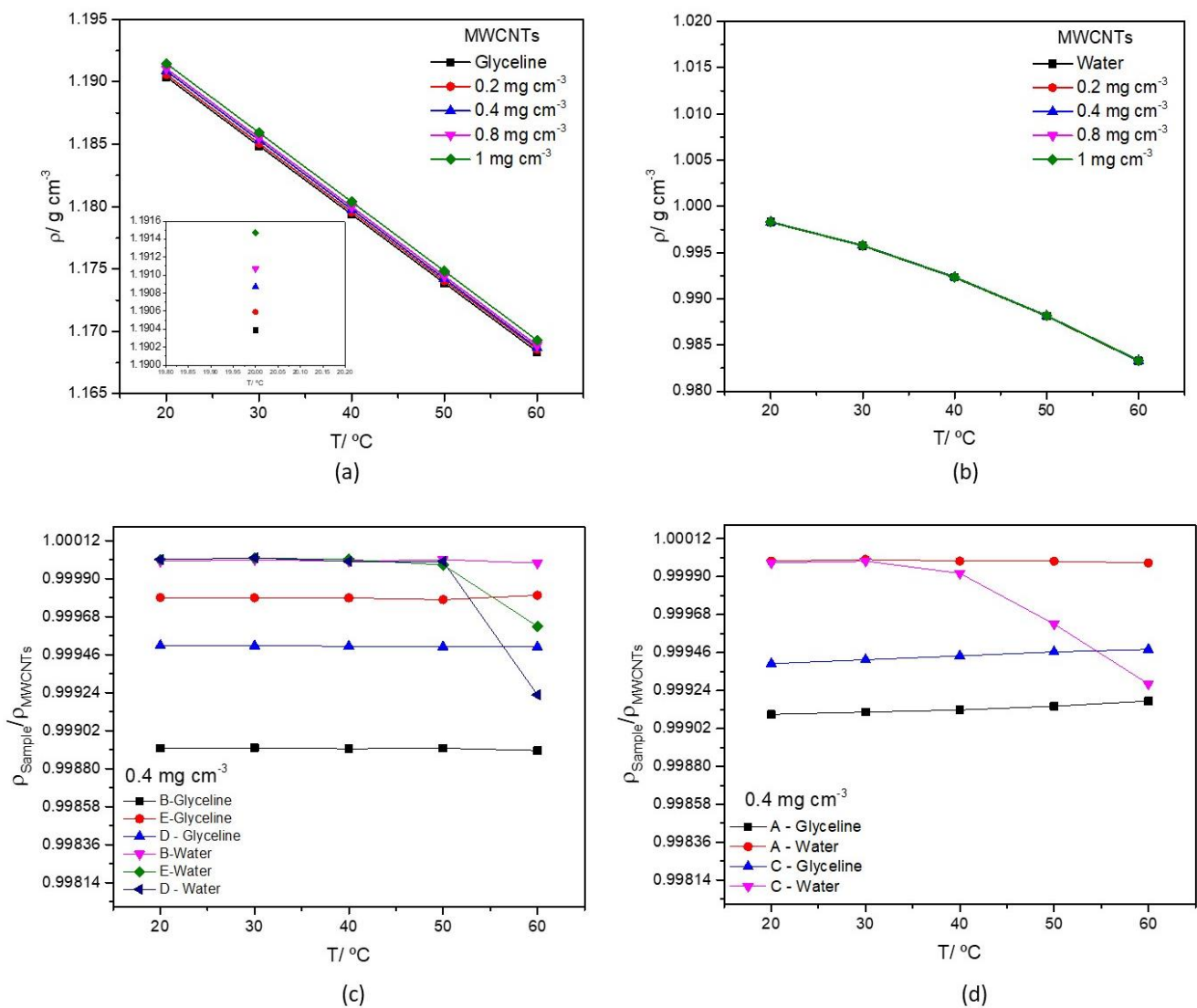
**Figure 3.** Densities of MWCNTs mixtures (0.2–1.0 mg cm$^{-3}$) in glyceline (**a**), water (**b**) as a function of temperature, and density ratio of AgMWCNTs (0.4 mg cm$^{-3}$) Samples B, D and E (**c**), A and C (**d**) as a function of temperature, in glyceline and water.

**Table 2.** Density values for glyceline and water at different temperatures (published and obtained results).

| Solvent | $\rho$/g cm$^{-3}$ | T/K | Reference | Solvent | $\rho$/g cm$^{-3}$ | T/K | Reference |
|---------|---------|-----|-----------|---------|---------|-----|-----------|
| | 1.198 | 293 | [27] | | 0.99829 | 293 | This work |
| | 1.190 | | This work | | 0.99821 | | [58] |
| glyceline | 1.180 | 298 | [59] | water | 0.99232 | 313 | This work |
| | 1.190 | | [60] | | 0.99222 | | [58] |
| | 1.130 | 363 | [60] | | 0.98329 | 333 | This work |
| | 1.190 | | [27] | | 0.98320 | | [58] |

Replacing MWCNTs by AgMWCNTs does not introduce any significant effect on the density of water dispersions (less than 0.01%). In glyceline, a slightly larger decrease in density is observed for all the samples in the temperature range between 20 and 60 °C (around 0.0633 ± 0.0003%).

### 3.3.2. Dynamic Viscosity

Viscosity is an important property that must be addressed, especially for equipment design and fluid flow calculations. Viscosity values for pure glyceline, found in the literature are listed in Table 3. The dynamic viscosity of ultrapure water is also in good agreement (less than 0.05% difference) with published values [58], indicating the quality of the measured values for glyceline and carbon dispersions.

**Table 3.** Dynamic viscosity values for glyceline and water at different temperatures (published and obtained results).

| Solvent | η/mPa s | T/K | Reference | Solvent | η/mPa s | T/K | Reference |
|---|---|---|---|---|---|---|---|
| glyceline | 497 | 293 | This work | Water | 1.0016 1.0074 | 293 | [58] This work |
| | 325 423 | 298 | [59] [60] | | 0.7972 0.8023 | 303 | [58] This work |
| | 259 | 303 | This work | | 0.6527 0.6604 | 313 | [58] This work |
| | 146 | 313 | This work | | | | |

The viscosity as a function of temperature is presented in Figure 4, for different concentrations of MWCNTs in glyceline and water (Figure 4a,b respectively). The viscosity of water is significantly lower than glyceline, and the decrease of viscosity with the increase in temperature is observed for both media, being more pronounced in glyceline (90% decrease from 20 °C to 60 °C).

The introduction of MWCNTs in the dispersing media displays a different behavior in glyceline and water. There is a decrease in viscosity in glyceline and an increase in water when adding MWCNTs, which is in agreement with data reported in some research papers [61,62]. That inversion observed in glyceline was previously reported by Alizadeh and Moraveji [63], for graphene nanoplatelets dispersed in an ionic liquid which showed a decrease in viscosity when compared to the original ionic liquid. This phenomenon might be explained by the self-lubricating nature of carbonous materials. Lower viscosity can result in reducing the pressure drop penalty in thermo-fluids systems and increasing the hydraulic and energy efficiency as a result [64].

The effect of Ag-NPs attached to the MWCNTs surface, dispersed in glyceline and water media is presented in Figure 4c (Samples B, D and E), 4d (Samples A and C). To facilitate data interpretation Figure 4c,d present the ratio of $\eta_{\text{Ag-M WCNTs}}/\eta_{\text{MWCNTs}}$ as a function of temperature for samples at a fixed concentration (0.4 mg cm$^{-3}$). The measured dynamic viscosity values of MWCNTs and AgMWCNTs dispersions (Samples A to E) as a function of temperature in the range 20 °C to 60 °C are presented in SI, in Figure S3f, Tables S6 and S7 for glyceline and Figure S4f, Tables S8 and S9 for water.

The introduction of AgMWCNTs on glyceline media leads to a small increase in viscosity when compared to pristine MWCNTs. AgMWCNTs dispersions in water display a systematic increase in viscosity (when compared to MWCNTs dispersions) of around 1.6%. When this study is carried out in glyceline, the AgMWCNTs samples containing larger amounts of silver (Samples B, D and E) display a decrease in viscosity (a 5.0% decrease) while dispersions prepared with Samples A and C show an increase in viscosity (a 6.7% increase). Samples D and E (which have a larger amount of Ag) display a larger and more consistent decrease in viscosity.

Studying the viscosity change with temperature allows to retrieve important information that can be retrieved by fitting an Arrhenius type Equation (1):

$$\ln \eta = \ln \eta_0 + \frac{E_\eta}{RT} \tag{1}$$

where $\eta_0$ is a constant, $E_\eta$ is the energy for activation of the viscous flow, R is the gas constant (8.31 J K$^{-1}$ mol$^{-1}$) and T is the temperature (K) [65]. Figure 5 shows that the data for MWCNTs dispersion in glyceline and water obey Equation (1) well ($R^2 > 0.989$).
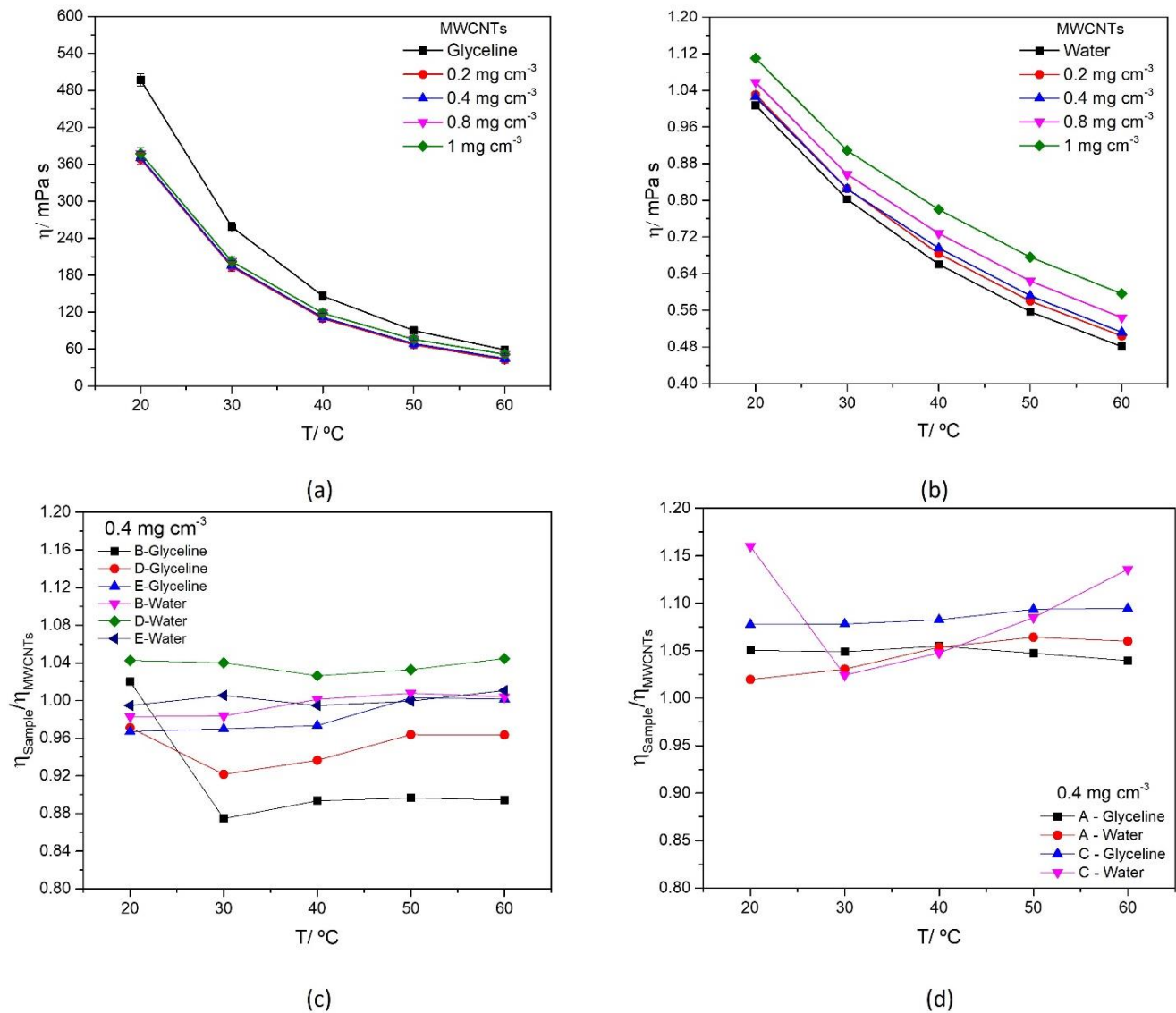


(a)

(b)

(c)

(d)

**Figure 4.** Dynamic viscosity of MWCNTs mixtures (0.2–1.0 mg cm$^{-3}$) in glyceline (**a**), water (**b**) as a function of temperature, and dynamic viscosity ratio of AgMWCNTs (0.4 mg cm$^{-3}$) Samples B, D and E (**c**), A and C (**d**)) as a function of temperature, in glyceline and water.

Tables 4 and 5 list the values of ln ($\eta_0$) (interception), $E_\eta$/R (slope), and the regression coefficient ($R^2$) the model for viscosity/temperature in glyceline and water, respectively. The minimum $R^2$ was 0.996, for the higher concentration of MWCNTs in glyceline and water.

The calculated values of $E_\eta$ are summarized in Tables S10 and S11, in Supplementary Materials, for glyceline and water, respectively. The values of $E_\eta$ diminish when the concentration of increases from 0.2 to 1.0 mg cm$^{-3}$. This effect is observed for all samples tested in this study. It is known that lower activation energy is associated with more mobile ions within the melt [66].
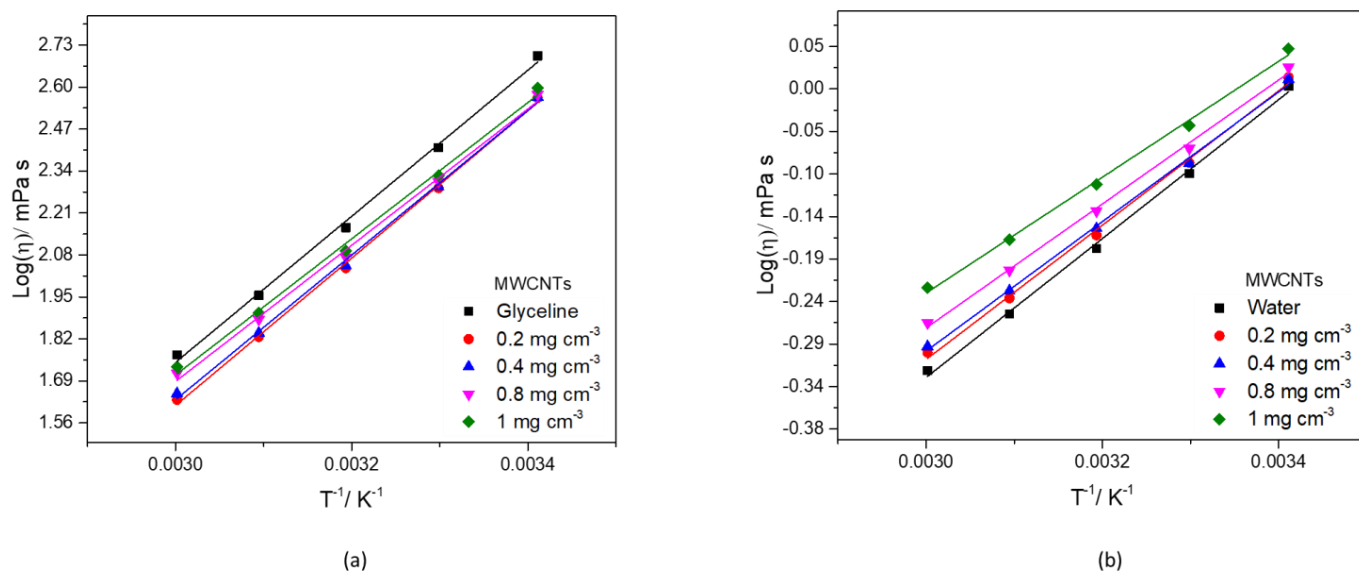
(a)



(b)

**Figure 5.** Plot of the logarithm of the viscosities against the reciprocal value of the absolute temperature for glyceline (**a**) and water (**b**) containing MWCNTs with different concentrations.

**Table 4.** Viscosity–temperature model parameters for MWCNTs dispersed in glyceline.

| | **Glyceline** | **MWCNTs Concentration/mg cm$^{-3}$** | | | |
| | | **0.2** | **0.4** | **0.8** | **1.0** |
|---|---|---|---|---|---|
| ln ($\eta_0$) | $-5.0 \pm 0.2$ | $-5.2 \pm 0.2$ | $-5.1 \pm 0.2$ | $-4.6 \pm 0.2$ | $-4.6 \pm 0.2$ |
| ($E_\eta$/R)/K | $2261 \pm 63$ | $2281 \pm 48$ | $2239 \pm 54$ | $2109 \pm 72$ | $2119 \pm 75$ |
| $R^2$ | 0.997 | 0.998 | 0.998 | 0.996 | 0.996 |

**Table 5.** Viscosity–temperature model parameters for MWCNTs dispersed in water.

| | **Water** | **MWCNTs Concentration/mg cm$^{-3}$** | | | |
| | | **0.2** | **0.4** | **0.8** | **1.0** |
|---|---|---|---|---|---|
| ln ($\eta_0$) | $-2.68 \pm 0.07$ | $-2.58 \pm 0.07$ | $-2.49 \pm 0.06$ | $-2.37 \pm 0.06$ | $-2.19 \pm 0.06$ |
| ($E_\eta$/R)/K | $784 \pm 21$ | $758 \pm 22$ | $732 \pm 18$ | $700 \pm 19$ | $654 \pm 20$ |
| $R^2$ | 0.997 | 0.997 | 0.998 | 0.997 | 0.996 |

Figures S3a–e and S4a–e, in Supplementary Materials, show the fitting data of AgMWCNTs dispersion in glyceline and water, respectively which obey Equation (1) well ($R^2 > 0.989$). The values of $E_\eta$ follow the same trend described for the MWCNTs dispersions, diminishing when the concentration increases from 0.2 to 1.0 mg cm$^{-3}$. Tables S12 and S13 list the values of ln ($\eta_0$) (interception), $E_\eta$/R (slope), and the regression coefficient ($R^2$) the model for viscosity/temperature in glyceline and water, respectively, for AgMWCNTs dispersions.

### 3.3.3. Surface Tension

The intermolecular attractive forces in a liquid result in cohesive tension that diminishes the surface area of the liquid's interface with other phases in contact with the liquid, a phenomenon identified as surface tension, which is measured as the energy required to increase the surface area of a liquid by a unit of area. Surface tension values for pure glyceline and water, found in the literature are listed in Table 6, presenting similar results.

The difference between the experimental values presented for glyceline with the ones reported in the literature may be attributed to a possible difference in the water content of DES however this cannot be verified since other authors did not provide that information.

**Table 6.** Surface tension values for glyceline and water at different temperatures (published and obtained results).

| Solvent | $\gamma$/mN m$^{-1}$ | T/K | Reference | Solvent | $\gamma$/mN m$^{-1}$ | T/K | Reference |
|---|---|---|---|---|---|---|---|
| | 57.80 56.33 | 293 | [67] This work | | - | - | - |
| | 68.10 59.01 | 298 | [59] [60] | | 71.19 71.54 | 303 | [58] This work |
| glyceline | 54.11 | 313 | This work | water | 69.60 69.88 | 313 | [58] This work |
| | 53.77 | 323 | This work | | 67.94 68.19 | 323 | [58] This work |
| | 53.31 | 333 | This work | | 64.48 65.43 | 333 | [58] This work |

Figure 6 shows the effect of concentration and temperature of MWCNTs in glyceline (Figure 6a) and water (Figure 6b). All measured surface tension values of MWCNTs and AgMWCNTs (Samples A to E) as a function of temperature are presented in Supplementary Materials, in Tables S14–S17, respectively for water and glyceline dispersions. Figure S5 presents the surface tension of glyceline/water mixtures with MWCNTs and Ag-MWCNTs as a function of carbon concentration (a) and temperature (b and c).
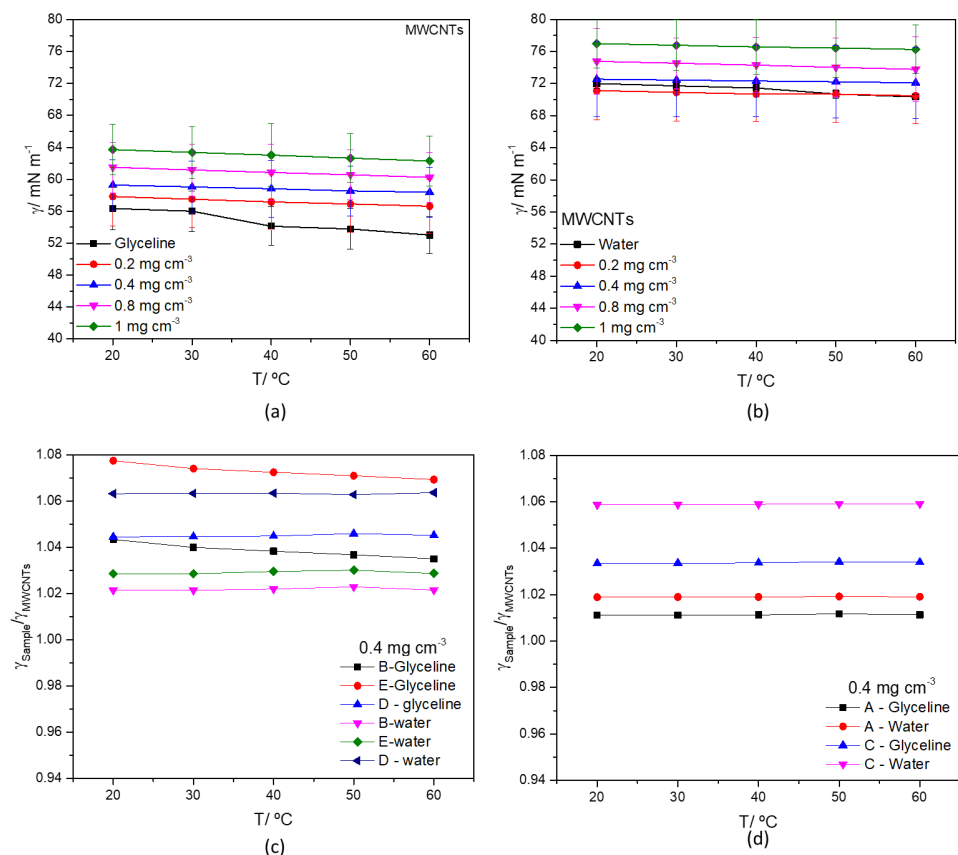


**Figure 6.** Surface tension of MWCNTs mixtures (0.2–1.0 mg cm$^{-3}$) in glyceline (**a**), water (**b**) as a function of temperature, and surface tension ratio of AgMWCNTs (0.4 mg cm$^{-3}$) Samples B, D and E (**c**) and A and C (**d**) as a function of temperature, in glyceline and water.

Figure 6a,b show that both tested solvents display a decrease in surface tension with increasing temperature. The same trend was reported by Abbott et al. [68], where the surface tension is strictly correlated with the viscosity of the system, which will be discussed later. The eight different MWCNTs dispersions (four in each solvent) display the same trend of the pure solvents (Figure 6a,b) showing an increase in surface tension with the increase in MWCNTs concentration. A similar effect was already reported in the literature [69] and is more pronounced in glyceline than in water and reflects the reduced surface activity of the MWCNTs dispersed in glyceline or water. Figure 6c (Samples B, D and E) and 6d (Samples A and C) present the ratio of $\gamma_{\text{Ag-M WCNTs}}/\gamma_{\text{MWCNTs}}$ as a function of temperature for AgMWCNTs dispersions at a fixed concentration (0.4 mg cm$^{-3}$). Dispersions of AgMWCNTs display a further increase in surface tension in water (between 2 and 6% increase) and in glyceline (between 1 and 7% increase).

Surface tension data, presented in Figure 6a,b, was analyzed using the "hole theory" developed by Abbott et al. [70,71]. DES "hole theory" was developed by Abbott based on the initial model developed by Fürth [72], which can be used to explain the mobility of ions/particles [70,71]. The "hole theory" model was also considered as a valid model by Bockris et al. [73] to describe high-temperature molten salts. According to this model [74], ionic materials contain empty spaces constituted from thermally generated fluctuations in local density. The vacancies are of random size and its position are in constant motion. It is assumed that an ion can only move through an ionic liquid if it is adjacent to a hole of equal or greater size. The average hole size, r, in a liquid is given by the Equation (2) [71]:

$$4\pi\langle r^2\rangle = 3.5\,\frac{k\,T}{\gamma} \tag{2}$$

where k is the Boltzmann constant, $\gamma$ is the surface tension, and T is the temperature. The results obtained for glyceline and MWCNTs dispersion are listed in Table 7.

**Table 7.** Average hole size (Å) according to the hole theory for pure glyceline and several dispersions prepared with increasing concentration of MWCNTs at different temperatures.

| | Glyceline | MWCNTs Concentration/mg cm$^{-3}$ | | | |
|---|---|---|---|---|---|
| T/°C | | 0.2 | 0.4 | 0.8 | 1.0 |
| 20 | 4.216 | 4.160 | 4.110 | 4.035 | 3.964 |
| 30 | 4.300 | 4.244 | 4.188 | 4.114 | 4.042 |
| 40 | 4.446 | 4.326 | 4.265 | 4.193 | 4.119 |
| 50 | 4.531 | 4.405 | 4.342 | 4.269 | 4.197 |
| 60 | 4.634 | 4.483 | 4.415 | 4.347 | 4.274 |

In the studied dispersions, taking into consideration the studied parameters (concentration, temperature, and presence of MWCNTs in glyceline) it is possible to verify, that the void radius decreases with the increase in the concentration of MWCNTs. The results were further compared with pure glyceline. At 20 °C, the DES presents a void radius of 4.216 Å, followed by the MWCNTs dispersion with 4.160 Å, at 0.2 mg cm$^{-3}$. The obtained values of void radius for the dispersion with MWCNTs in glyceline are lower than the carbon-free liquid, indicating that the viscosity decrease is probably controlled by the lubricating properties of MWCNTs [63] rather than the hole size [71].

The values for the average hole size, r, for the AgMWCNTs in glyceline, are presented in Tables S18 and S19 in the Supplementary Materials, revealing that the void radius increases when AgMWCNTs dispersions are used. However, this increase in the void radius is not reflected in a general decrease in viscosity, when compared to MWCNTs dispersions. Samples A and C show an increase in viscosity (Figure 4d) and Samples B, D and E (Figure 4c) show a decrease in viscosity. The presence of AgNPs at MWCNTs surface altered the force balance introducing new surface interactions with the DES components that reduced the MWCNTs lubricating properties but potentiate the increase in the void

size. It is the delicate balance between these two opposite effects that define the effect over the dispersion average viscosity.

### 3.3.4. Ionic Conductivity

Electrochemical applications are an important field where DESs can have a significant contribution to the industry, so there is a great demand for information concerning their electrical and electronic properties, including their ionic conductivity. Due to their relatively high viscosity, DESs have low conductivity. In general, the conductivity of DESs increases as temperature increases [59].

Ionic conductivity values for pure glyceline and water, found in the literature are listed in Table 8. The values for ultrapure water is also in good agreement (less than 1.5% difference) with published values [58]. The ionic conductivity presented by the Milli-Q® water manufacturer is also in good agreement with the obtained result at 20 °C.

The difference between the experimental values presented for glyceline with those reported in the literature may be attributed to a possible difference in the water content of DES this information could not be found and the presence of water in the eutectic mixture can help increase the conductivity [75].

**Table 8.** Ionic conductivity values for glyceline and water at different temperatures (published and obtained results).

| Solvent | $\sigma$/mS cm$^{-1}$ | T/K | Reference | Solvent | $\sigma$/$\mu$S cm$^{-1}$ | T/K | Reference |
|---|---|---|---|---|---|---|---|
| glyceline | 0.413 | 293 | This work | water | 0.045 | 293 | [58] |
| | | | | | 0.050 | | This work |
| | 2.039 | 298 | [59] | | 0.056 | | Milli-Q® water * |
| | 0.981 | | [60] | | | | |
| | 0.850 | | [76] | | 0.061 | 303 | [58] |
| | | | | | 0.055 | | This work |
| | 0.433 | 303 | This work | | | | |
| | | | | | 0.070 | 313 | [58] |
| | 1.501 | 313 | This work | | 0.061 | | This work |
| | 1.914 | 323 | This work | | 0.075 | 323 | [58] |
| | | | | | 0.067 | | This work |
| | 3.099 | 333 | This work | | | | |
| | 3.441 | | [76] | | 0.083 | 333 | [58] |
| | | | | | 0.071 | | This work |
| | 7.652 | 343 | [59] | | | | |
| | 4.520 | | [60] | | | | |

* https://www.merckmillipore.com/PT/en/product/Milli-Q-Reference-Water-Purification-System,MM_NF-Z00QSV0WW. (Last accessed at 10 November 2021).

The conductivity as a function of temperature is represented in Figure 7, for different concentrations of MWCNTs in glyceline and water (Figure 7a,b respectively). For all the measurements, with increasing temperature, there is an increase in ionic conductivity.

The ionic conductivity of MWCNTs and AgMWCNTs mixtures (samples A to E) as a function of temperature in the range 20 °C to 60 °C are presented in Supplementary Materials, in Tables S20 and S21 and Tables S22 and S23, respectively for water and glyceline.

For all the MWCNTs measurements, in both glyceline and water, with increasing temperature, there is an increase in conductivity. Several studies have presented a considerable increase in conductivity of the fluids with the addition and dispersion of graphene NPs to them [77,78]. The increase of conductivity with the suspension of carbon materials, in this case, MWCNTs, can be attributed to the charge transfer enhancement which is significantly affected by EDL (electrical double layer) effect in solution [79].
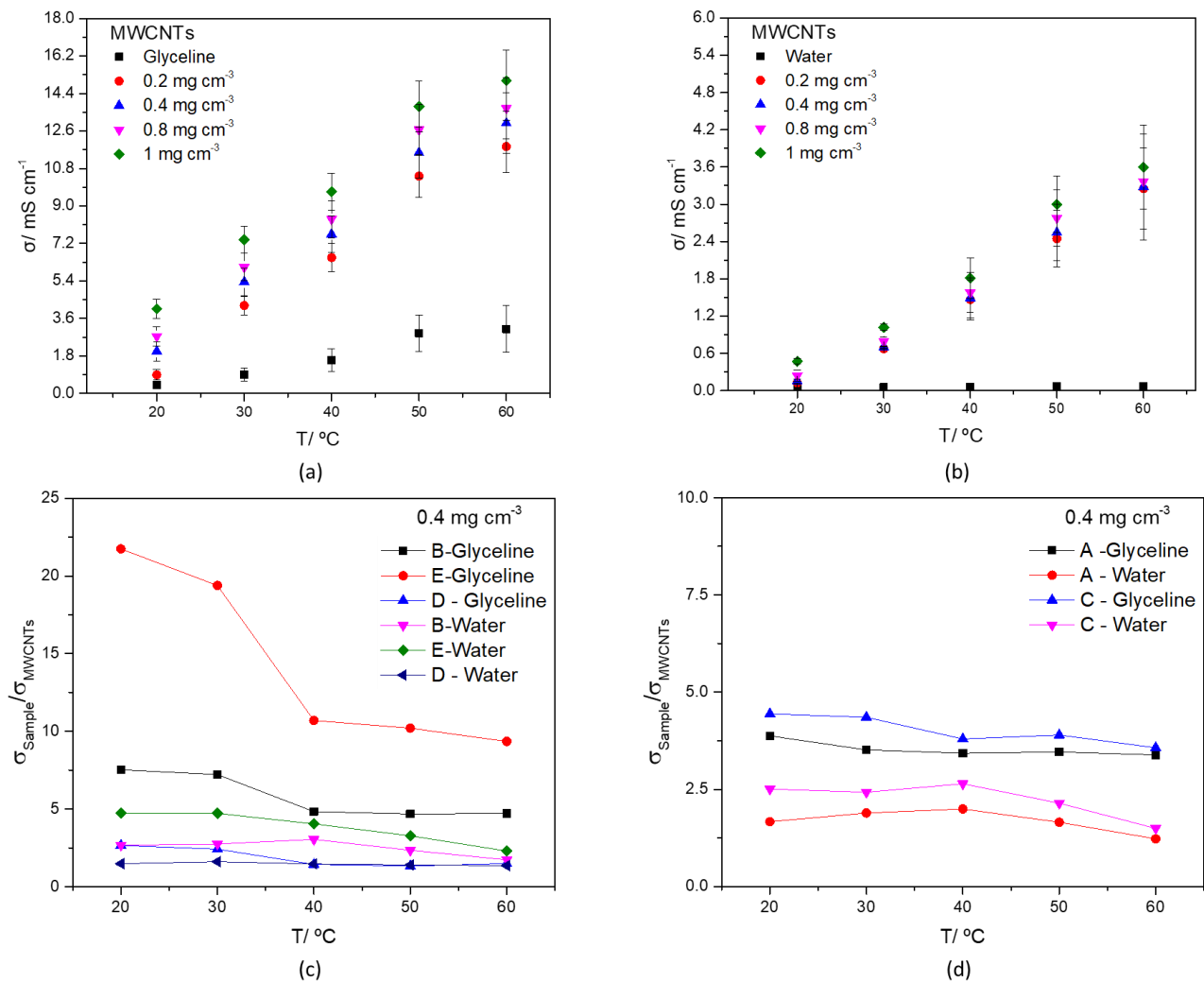
**Figure 7.** Ionic conductivity of MWCNTs mixtures (0.2–1.0 mg cm$^{-3}$) in glyceline (**a**), water (**b**) as a function of temperature, and ionic conductivity ratio of AgMWCNTs (0.4 mg cm$^{-3}$) Samples B, D and E (**c**) and A and C (**d**) as a function of temperature, in glyceline and water.

The effect of Ag-NPs attached to the MWCNTs surface, dispersed in glyceline and water media is presented in Figure 7c (Samples B, D, and E) and 7d (Samples A, and C). To facilitate data interpretation Figure 7c,d present the ratio of $\sigma_{AgMWCNTs}/\sigma_{MWCNTs}$ as a function of temperature for samples at a fixed concentration (0.4 mg cm$^{-3}$).

The effect of the presence of the Ag-NPs is very pronounced in this physicochemical property, especially in the glyceline media, showing a decrease in the effect of the Ag-NPs with an increase in temperature. As expected (Figures S6f and S7f, in Supplementary Materials), the Ag-NPs were able to contribute to a substantial increase of the ionic conductivity of dispersion media containing AgMWCNTs due to the high conductivity of silver (r$_{Ag}$ = 6.30 × 10$^5$ S cm$^{-1}$) [17].

The ionic conductivity changes, by the introduction of AgMWCNTs, presents an increase up to 20 times, compared to MWCNTs, especially in the sample with a higher amount and size of Ag-NPs (Sample E), followed by the samples with a lower amount of Ag NPs, showing that both parameters are strictly correlated with the ionic conductivity. The increase in conductivity brought by the attachment of Ag-NPs to the MWCNTs surface was also presented earlier [17,80–83].

The effect of temperature on the conductivity can be described according to Arrhenius-type behavior (log σ vs. 1/T), as previously developed by Abbott et al. [68,76] and presented in Equation (3).

$$\ln \sigma = \ln \sigma_0 - \frac{E_\sigma}{RT} \tag{3}$$

where σ is the conductivity at temperature T (K), $\sigma_0$ is the corresponding pre-exponential factor, $E_\sigma$ is the activation energy of ionic conductivity and R is the gas constant (8.31 J K$^{-1}$ mol$^{-1}$). Figure 8a,b show that the data fits Equation (3) accurately ($R^2 > 0.998$).



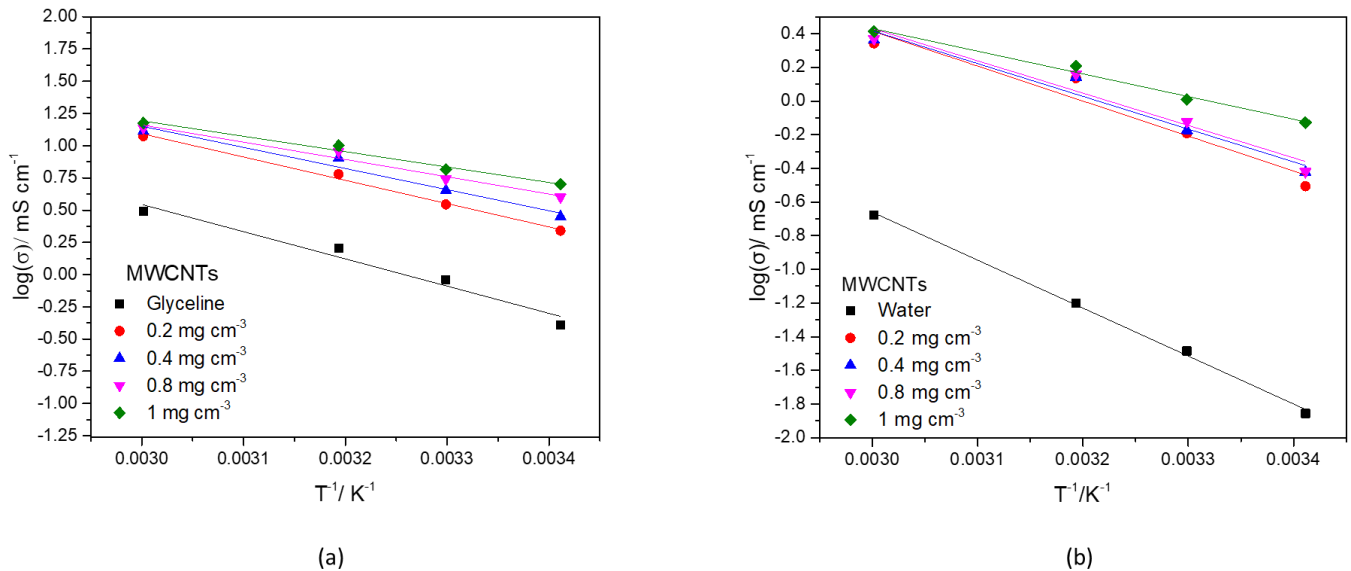(a)                                              (b)

**Figure 8.** Plot of the logarithm of the conductivity against the reciprocal value of the absolute temperature (1/T) for glyceline (**a**) and water (**b**) containing MWCNTs with different concentrations.

Tables 9 and 10 lists the values of ln ($\sigma_0$) (interception), $E_\sigma$/R (slope), and the regression coefficient ($R^2$) the model for conductivity/temperature in glyceline and water, respectively. The minimum $R^2$ was 0.972, for the higher concentrations of MWCNTs in glyceline.

**Table 9.** Conductivity–temperature model parameters for MWCNTs dispersed in glyceline.

|  | MWCNTs Concentration/mg cm$^{-3}$ | | | | |
|---|---|---|---|---|---|
|  | **Glyceline** | **0.2** | **0.4** | **0.8** | **1.0** |
| ln ($\sigma_0$) | $6.9 \pm 0.9$ | $6.5 \pm 0.3$ | $6.1 \pm 0.6$ | $5.2 \pm 0.5$ | $4.8 \pm 0.4$ |
| ($E_\sigma$/R)/K | $-2111 \pm 274$ | $-1806 \pm 85$ | $-1638 \pm 193$ | $-1340 \pm 144$ | $-1194 \pm 110$ |
| $R^2$ | 0.989 | 0.991 | 0.979 | 0.977 | 0.972 |

**Table 10.** Conductivity–temperature model parameters for MWCNTs dispersed in water.

|  | MWCNTs Concentration/mg cm$^{-3}$ | | | | |
|---|---|---|---|---|---|
|  | **Water** | **0.2** | **0.4** | **0.8** | **1.0** |
| ln ($\sigma_0$) | $7.9 \pm 0.3$ | $7 \pm 1$ | $6.3 \pm 0.9$ | $6 \pm 1$ | $4.5 \pm 0.3$ |
| ($E_\sigma$/R)/K | $-2848 \pm 95$ | $-2076 \pm 366$ | $-1945 \pm 286$ | $-1921 \pm 308$ | $-1347 \pm 104$ |
| $R^2$ | 0.997 | 0.981 | 0.979 | 0.982 | 0.991 |

The activation energy of ionic conductivity for the Samples A to E, in glyceline and water, are presented in Table S10 and S11, in Supplementary Materials. The $E_\sigma$ of water is higher, for all MWCNTs concentrations than glyceline. In both cases, there is a decrease in the $E_\sigma$ with an increase in MWCNTs concentration.

Figures S6 and S7 show the fitting data for AgMWCNTs dispersion in glyceline and water, respectively which fits Equation (3) accurately ($R^2 > 0.998$). The presence of AgNPs in the MWCNTs significantly improves the Arrhenius-type behavior of glyceline ionic conductivity. Tables S24 and S25 list the values of ln ($\sigma_0$) (interception), $E_\sigma/R$ (slope), and the regression coefficient ($R^2$) the model for conductivity/temperature in glyceline and water, respectively, for AgMWCNTs dispersions.

Since the conductivity is controlled by the mobility of the charge carriers in ionic fluids, the plot of $E_\sigma$ vs. $E_\eta$ should be linear [68]. That is visible in Figure 9a, for glyceline, containing MWCNTs and AgMWCNTs. However, the same cannot be observed in water, presented in Figure 9b, since it is not an ionic fluid, as presented by Abbott et al. [68].
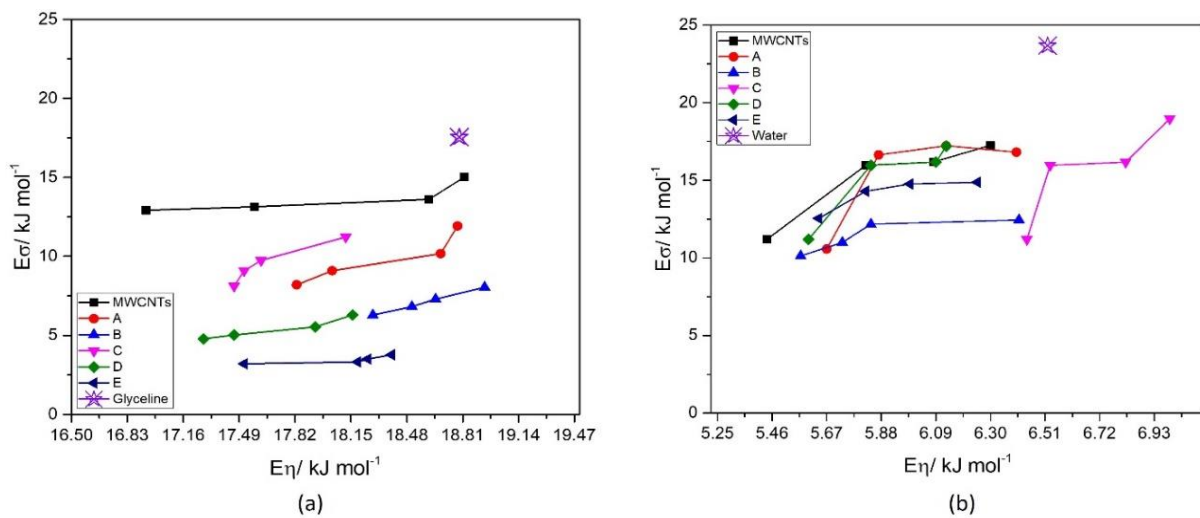


(a)　　　　　　　　　　　　　　　　　　　　　　　(b)

**Figure 9.** Activation energy of conductivity as a function of activation energy of viscosity for MWCNTs and AgMWCNTs (Samples A to E) in glyceline (**a**) and water (**b**).

### 3.3.5. Refractive Index

The experimental refractive index (RI) data in glyceline and water at room temperature, at different concentrations of MWCNTs, is presented in Figure 10a,b, respectively. Refractive index values for pure glyceline and water, found in the literature are listed in Table 11.

**Table 11.** Refractive index values for glyceline and water at different temperatures (published and obtained results).

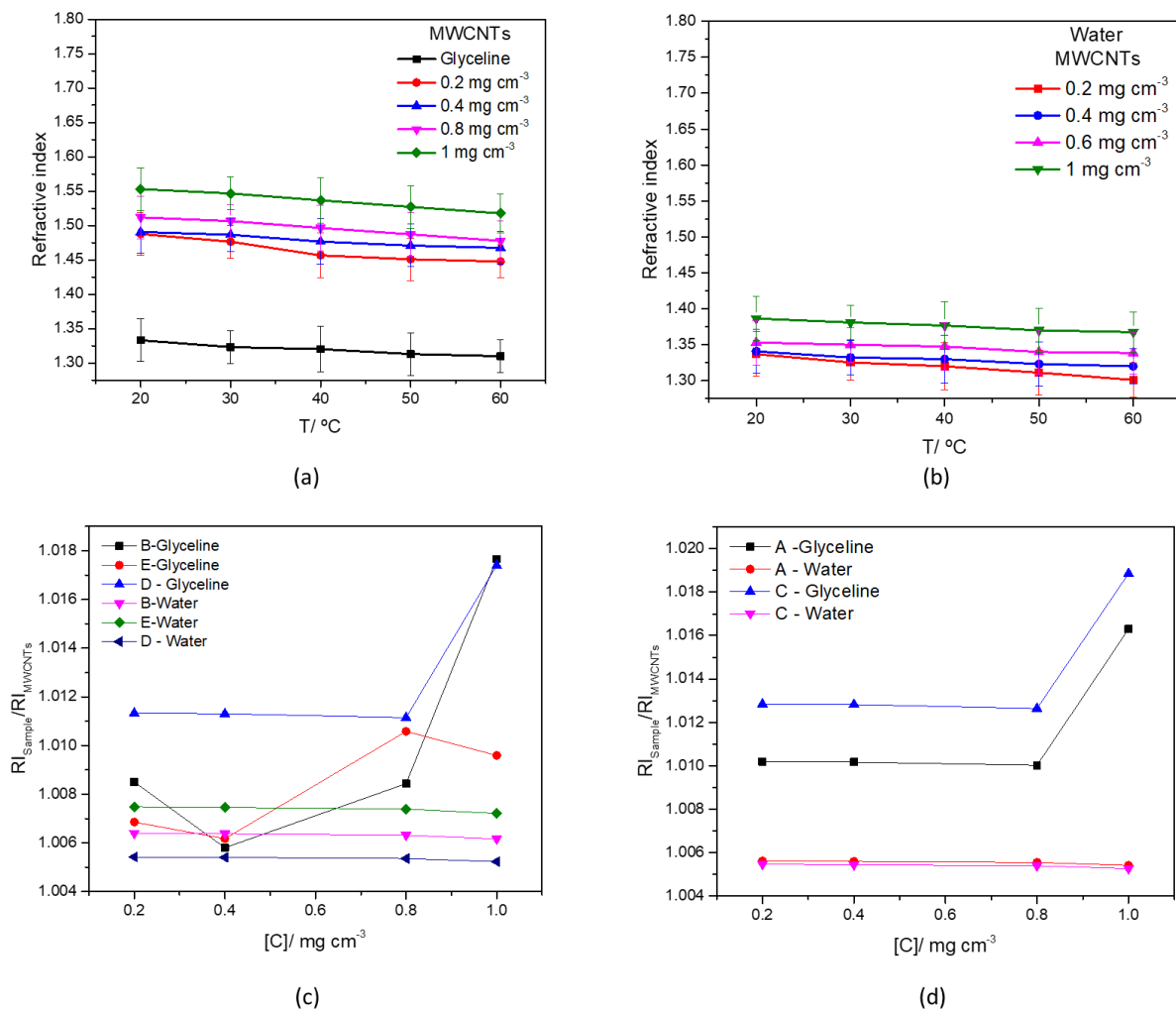| Solvent | RI | T/K | Reference | Solvent | RI | T/K | Reference |
|---|---|---|---|---|---|---|---|
|  | 1.3331 | 293 | This work |  | 1.3321 | 293 |  |
|  | 1.3325 | 298 | [84] |  | 1.3310 | 298 |  |
|  | 1.3231 |  | This work |  |  |  |  |
|  | 1.3319 | 303 | [84] |  | 1.3242 | 303 |  |
| glyceline | 1.3201 | 313 | This work | water | 1.3229 | 313 | [58] |
|  | 1.3305 |  | [84] |  |  |  |  |
|  | 1.3131 | 323 | This work |  | 1.3214 | 323 |  |
|  | 1.3289 |  | [84] |  |  |  |  |
|  | 1.3099 | 333 | This work |  | 1.3197 | 333 |  |
|  | 1.3269 |  | [84] |  |  |  |  |

**Figure 10.** Refractive index of MWCNTs mixtures (0.2–1.0 mg cm$^{-3}$) in glyceline (**a**), water (**b**) as a function of temperature, and refractive index ratio of AgMWCNTs (0.4 mg cm$^{-3}$) Samples B, D and E (**c**) and A and C (**d**) as a function of concentration, in glyceline and water.

The measured refractive index values of MWCNTs AgMWCNTs mixtures (Samples A to E) as a function of temperature in the range 20 °C to 60 °C, and concentration are presented in Supplementary Materials, in Tables S26–S29, respectively for water and glyceline. Figure S8 presents the effect of concentration of MWCNTs and AgMWCNTs composites on refractive index in glyceline (a) and water (b) media, at 20 °C.

An increase in the concentration of MWCNTs is associated with an increase in the RI, in both glyceline and water. This can be rationalized by the fact that by increasing the concentration of MWCNTs, the availability of carbon materials in solution increases, raising the chances of light to hit a higher number of molecules, and thereby increasing the RI [81]. The effect of temperature was performed for MWCNTs in both glyceline and water, showing that increasing the temperature, the molecules speed increases in solution, causing the light to hit fewer molecules, and thereby reducing the RI [82,83].

The increasing trend of RI with increasing concentration of MWCNTs is also found in the literature [67]. The experimental RI data in glyceline and water at room temperature, at different concentrations of MWCNTs and AgMWCNTs, is presented in Figure S8. It can be observed that the increase in the concentration of MWCNTs and AgMWCNTs is associated with an increase in the RI, in both glyceline and water.

The effect of Ag-NPs attached to the MWCNTs surface, dispersed in glyceline and water media can be observed by analysis of Figure 10c (Samples B, D and E), 10d (Samples

A and C). To facilitate data interpretation, Figure 10c,d present the ratio of $RI_{AgM\ WCNTs}/RI_{MWCNTs}$ as a function of temperature for samples at a fixed concentration (0.4 mg cm$^{-3}$).

Shahriari et al. [85] concluded that, with the growth of Ag-NPs size, there is an increase of the RI, due to the increase of diffusivity of the medium. That correlation can be observed for the AgMWCNTs samples in glyceline, especially for Samples B, C and D; however, it was expected that behavior for Sample E, which presents the bigger size of AgNPs, and that is not the case.

### 3.4. Statistical Analysis

The analysis of variance through two-way ANOVA, for viscosity, density, conductivity, and surface tension, as a function of the concentration of MWCNTs and AgMWCNTs (Samples A to E), are shown in Tables S30 and S31, in Supplementary Materials, for glyceline and water, respectively, with 5% level of significance. The statistical significance of the different studied physicochemical parameters depends on the $p$-value.

Starting with the analysis of the results from glyceline media, the concentration of both MWCNTs and AgMWCNTs is statistically significant in defining the properties of viscosity, conductivity, and surface tension, while the effect of temperature is statistically significant in all the studied parameters, presenting a $p$-value < 0.05. The interaction between concentration and temperature is statistically significant only in conductivity and surface tension.

The same conclusions cannot be taken when referring to water media. The effect of concentration and temperature on viscosity, density and conductivity are not statistically significant ($p$-value > 0.05), as proved by the experimental data, meaning that other experimental factors that were not considered in this study are affecting the physicochemical properties under evaluation. The only parameter in which both factors are statistically significant, including its interaction, is the surface tension, with a $p$-value < 0.0001.

For both dispersion media, the statistical analysis corroborates the experimental data obtained in this work.

## 4. Conclusions

The effect of MWCNTs and AgMWCNTs composites on the physicochemical properties of choline chloride-based DES, glyceline, and water was investigated, in the range of concentration from 0.2 to 1.0 mg cm$^{-3}$. The experimental results could be interpreted in terms of the hole theory, in which the ion transfer in DES is limited by the availability of holes of suitable size within the structure of the liquid, nevertheless, the effect of MWCNTs on viscosity and conductivity cannot be explained solely in terms of the hole theory and the contribution of the self-lubricating nature of carbonous materials has to be considered to explain the experimental results.

The measurements of viscosity, density, conductivity, surface tension and refractive index have been conducted. An increase in temperature was shown to result in a decrease in viscosity, density, and surface tension. The conductivity increases with an increase in temperature since it is controlled by ionic mobility.

The introduction of MWCNTs dispersions to glyceline and water led to an increase in conductivity, surface tension and refraction index. However, in glyceline, the presence of carbon nanomaterials led to a decrease in viscosity. The same study carried out in water led to an increase in viscosity, proving the exceptional properties of this choline chloride-based DES.

In general, the use of AgMWCNTs leads to a slight improvement of the dispersion properties, when compared to the use of MWCNTs dispersions. Conductivity is the physicochemical property that benefits the most from the use of AgMWCNTs, allowing to achieve up to 20 × enhancement of conductivity when MWCNTs dispersions are replaced by AgMWCNTs dispersions.

The dispersion of MWCNTs and AgMWCNTs is an exciting area of future research, in particular, their dispersion in eutectic mixtures. The obtained physicochemical properties

of the MWCNTs/AgMWCNTs-glyceline dispersions will path the way to achieve exciting breakthroughs in carbon dispersions in the coming years, for several applications, especially in solid-state electrolytes and electrodes for energy storage devices.

**Supplementary Materials:** The following supporting information can be downloaded at: https://www.mdpi.com/article/10.3390/nano12010099/s1, Table S1: parameters for the electrodeposition process of AgMWCNTs. Data from Brandão et al. [24] ** Figure S1: densities ($\rho$/g cm$^{-3}$) of A–E mixtures (a–e) and comparison between samples at 0.4 mg cm$^{-3}$ (f) in glyceline as a function of temperature; Table S2: densities of MWCNTs and AgMWCNTs mixtures in glyceline as a function of temperature for 0.4 mg cm$^{-3}$; Table S3: densities of MWCNTs mixtures (0.2–1.0 mg cm$^{-3}$) in glyceline as a function of temperature; Figure S2: densities ($\rho$/g cm$^{-3}$) of A–E mixtures (a–e) and comparison between samples at 0.4 mg cm$^{-3}$ (f) in water as a function of temperature; Table S4: densities of MWCNTs and AgMWCNTs mixtures in water as a function of temperature for 0.4 mg cm$^{-3}$; Table S5: densities of MWCNTs mixtures (0.2–1.0 mg cm$^{-3}$) in water as a function of temperature; Figure S3: plot of logarithm of the viscosity against the reciprocal value of the absolute temperature (1/T) for of A–E mixtures (a–e) and comparison between samples at 0.4 mg cm$^{-3}$ (f) in glyceline; Table S6: viscosity of MWCNTs and AgMWCNTs mixtures in glyceline as a function of temperature for 0.4 mg cm$^{-3}$; Table S7: viscosity of MWCNTs mixtures (0.2–1.0 mg cm$^{-3}$) in glyceline as a function of temperature; Figure S4: plot of logarithm of the viscosity against the reciprocal value of the absolute temperature (1/T) for of A–E mixtures (a–e) and comparison between samples at 0.4 mg cm$^{-3}$ (f) in water; Table S8: viscosity of MWCNTs and AgMWCNTs mixtures in water as a function of temperature for 0.4 mg cm$^{-3}$; Table S9: viscosity of MWCNTs mixtures (0.2–1.0 mg cm$^{-3}$) in water as a function of temperature; Table S10: the calculated values of the activation energies of viscous flow ($E_\eta$) and conductivity ($E\tau$) at different concentrations of MWCNTs and AgMWCNTs composites (A–E), in glyceline; Table S11: the calculated values of the activation energies of viscous flow ($E_\eta$) and conductivity ($E\tau$) at different concentrations of MWCNTs and AgMWCNTs composites (A–E), in water.; Table S12: viscosity–temperature model parameters for AgMWCNTs samples dispersed in glyceline; Table S13: viscosity–temperature model parameters for AgMWCNTs samples dispersed in water; Table S14: surface tension of MWCNTs mixtures (0.2–1.0 mg cm$^{-3}$) in water as a function of temperature; Table S15: surface tension of MWCNTs and AgMWCNTs mixtures in water as a function of temperature for 0.4 mg cm$^{-3}$; Table S16: surface tension of MWCNTs mixtures (0.2–1.0 mg cm$^{-3}$) in glyceline as a function of temperature; Table S17: surface tension of MWCNTs and AgMWCNTs mixtures in glyceline as a function of temperature for 0.4 mg cm$^{-3}$; Figure S5: surface tension of glyceline/water mixtures with MWCNTs and AgMWCNTs as a function of carbon concentration (a) and temperature (b and c); Table S18: average hole size (Å) according to the hole theory for glyceline at different concentrations of AgMWCNTs composites (A–E) at 20 °C; Table S19: average hole size (Å) according to the hole theory for glyceline at different temperatures (20–60 °C) of AgMWCNTs composites (A–E) at 0.4 mg cm$^{-3}$; Table S20: conductivity of MWCNTs mixtures (0.2–1.0 mg cm$^{-3}$) in water as a function of temperature; Table S21: conductivity of MWCNTs and AgMWCNTs mixtures in water as a function of temperature for 0.4 mg cm$^{-3}$; Table S22: conductivity of MWCNTs mixtures (0.2–1.0 mg cm$^{-3}$) in glyceline as a function of temperature; Table S23: conductivity of MWCNTs and AgMWCNTs mixtures in glyceline as a function of temperature for 0.4 mg cm$^{-3}$; Figure S6: plot of logarithm of the conductivity against the reciprocal value of the absolute temperature (1/T) for of A–E mixtures (a–e) and comparison between samples at 0.4 mg cm$^{-3}$ (f) in glyceline; Figure S7: plot of logarithm of the conductivity against the reciprocal value of the absolute temperature (1/T) for of A–E mixtures (a–e) and comparison between samples at 0.4 mg cm$^{-3}$ (f) in water; Table S24: conductivity–temperature model parameters for AgMWCNTs samples dispersed in glyceline; Table S25: conductivity–temperature model parameters for AgMWCNTs samples dispersed in water; Table S26: refractive index of MWCNTs mixtures (0.2–1.0 mg cm$^{-3}$) in water as a function of temperature; Table S27: refractive index of MWCNTs and AgMWCNTs mixtures in water as a function of concentration at 20 °C; Table S28: refractive index of MWCNTs mixtures (0.2–1.0 mg cm$^{-3}$) in glyceline as a function of temperature; Table S29: refractive index of MWCNTs and AgMWCNTs mixtures in glyceline as a function of concentration at 20 °C; Figure S8: effect of concentration of MWCNTs and AgMWCNTs composites on refractive index in glyceline (a) and water (b) media, at 20 °C; Table S30: two-way ANOVA between the groups of MWCNTs and AgMWCNTs samples dispersed in glyceline with different temperatures (20–60 °C) and concentrations (0–1.0 mg cm$^{-3}$);

Table S31: two-way ANOVA between the groups of MWCNTs and AgMWCNTs samples dispersed in water with different temperatures (20–60 °C) and concentrations (0–1.0 mg cm$^{-3}$).

**Author Contributions:** Conceptualization, A.T.S.C.B. and C.M.P.; methodology, A.T.S.C.B. and C.M.P.; formal analysis, A.T.S.C.B. and C.M.P.; investigation, A.T.S.C.B., R.C., S.R. and C.M.P.; writing—original draft, A.T.S.C.B.; writing—review and editing, A.T.S.C.B., S.R., R.C., L.A., M.E. and C.M.P.; supervision: A.F.S., L.A., M.E. and C.M.P.; resources, M.E. and C.M.P.; funding acquisition, M.E. and C.M.P. All authors have read and agreed to the published version of the manuscript.

**Institutional Review Board Statement:** Not applicable.

**Informed Consent Statement:** Not applicable.

**Data Availability Statement:** Not applicable.

**Conflicts of Interest:** The authors declare no conflict of interest.

# References

1. Iijima, S. Helical microtubules of graphitic carbon. *Nature* **1991**, *354*, 56. [CrossRef]
2. Wu, T.-M.; Lin, Y.-W. Doped polyaniline/multi-walled carbon nanotube composites: Preparation, characterization and properties. *Polymer (Guildf.)* **2006**, *47*, 3576–3582. [CrossRef]
3. Ahmadpoor, F.; Zebarjad, S.M.; Janghorban, K. Decoration of multi-walled carbon nanotubes with silver nanoparticles and investigation on its colloid stability. *Mater. Chem. Phys.* **2013**, *139*, 113–117. [CrossRef]
4. Hoyos-Palacio, L.M.; Cuesta Castro, D.P.; Ortiz-Trujillo, I.C.; Botero Palacio, L.E.; Galeano Upegui, B.J.; Escobar Mora, N.J.; Carlos Cornelio, J.A. Compounds of carbon nanotubes decorated with silver nanoparticles via in-situ by chemical vapor deposition (CVD). *J. Mater. Res. Technol.* **2019**, *8*, 5893–5898. [CrossRef]
5. Georgakilas, V.; Gournis, D.; Tzitzios, V.; Pasquato, L.; Guldi, D.M.; Prato, M. Decorating carbon nanotubes with metal or semiconductor nanoparticles. *J. Mater. Chem.* **2007**, *17*, 2679–2694. [CrossRef]
6. Mousavi-Kamazani, M.; Salavati-Niasari, M. A simple microwave approach for synthesis and characterization of Ag$_2$S–AgInS$_2$ nanocomposites. *Compos. Part B Eng.* **2014**, *56*, 490–496. [CrossRef]
7. Cozzarini, L.; Bertolini, G.; Šuran-Brunelli, S.T.; Radivo, A.; Bracamonte, M.V.; Tavagnacco, C.; Goldoni, A. Metal decorated carbon nanotubes for electrocatalytic water splitting. *Int. J. Hydrogen Energy* **2017**, *42*, 18763–18773. [CrossRef]
8. Duc Chinh, V.; Speranza, G.; Migliaresi, C.; Van Chuc, N.; Minh Tan, V.; Phuong, N.-T. Synthesis of Gold Nanoparticles Decorated with Multiwalled Carbon Nanotubes (Au-MWCNTs) via Cysteaminium Chloride Functionalization. *Sci. Rep.* **2019**, *9*, 5667. [CrossRef]
9. Guzsvány, V.; Vajdle, O.; Gurdeljević, M.; Kónya, Z. Ag or Au Nanoparticles Decorated Multiwalled Carbon Nanotubes Coated Carbon Paste Electrodes for Amperometric Determination of H$_2$O$_2$. *Top. Catal.* **2018**, *61*, 1350–1361. [CrossRef]
10. Amiri, A.; Shanbedi, M.; Eshghi, H.; Heris, S.Z.; Baniadam, M. Highly Dispersed Multiwalled Carbon Nanotubes Decorated with Ag Nanoparticles in Water and Experimental Investigation of the Thermophysical Properties. *J. Phys. Chem. C* **2012**, *116*, 3369–3375. [CrossRef]
11. Tang, L.; Duan, F.; Chen, M. Silver nanoparticle decorated polyaniline/multiwalled super-short carbon nanotube nanocomposites for supercapacitor applications. *RSC Adv.* **2016**, *6*, 65012–65019. [CrossRef]
12. Patole, A.; Lubineau, G. Carbon nanotubes with silver nanoparticle decoration and conductive polymer coating for improving the electrical conductivity of polycarbonate composites. *Carbon N. Y.* **2015**, *81*, 720–730. [CrossRef]
13. Dinh, N.X.; Van Quy, N.; Huy, T.Q.; Le, A.T. Decoration of silver nanoparticles on multiwalled carbon nanotubes: Antibacterial mechanism and ultrastructural analysis. *J. Nanomater.* **2015**, *16*, 63. [CrossRef]

14. Markoulidis, F.; Todorova, N.; Grilli, R.; Lekakou, C. Trapalis Composite Electrodes of Activated Carbon and Multiwall Carbon Nanotubes Decorated with Silver Nanoparticles for High Power Energy Storage. *J. Compos. Sci.* **2019**, *3*, 97. [CrossRef]

15. Kharisov, B.I.; Kharissova, O.V.; Ortiz Méndez, U.; De La Fuente, I.G. Decoration of Carbon Nanotubes with Metal Nanoparticles: Recent Trends. *Synth. React. Inorg. Met. Nano-Met. Chem.* **2015**, *46*, 55–76. [CrossRef]

16. Travessa, D.N.; Da Silva, F.S.; Cristovan, F.H.; Jorge, A.M.; Cardoso, K.R. Ag ion decoration for surface modifications of multi-walled carbon nanotubes. *Mater. Res.* **2014**, *17*, 687–693. [CrossRef]

17. Xin, F.; Li, L. Decoration of carbon nanotubes with silver nanoparticles for advanced CNT/polymer nanocomposites. *Compos. Part A Appl. Sci. Manuf.* **2011**, *42*, 961–967. [CrossRef]

18. Cojocaru, A.; Brincoveanu, O.; Pantazi, A.; Balan, D.; Enachescu, M.; Visan, T.; Anicai, L. Electrochemical preparation of Ag nanoparticles involving choline chloride-glycerol deep eutectic solvents. *Bulg. Chem. Commun.* **2017**, *49*, 194–204.

19. Kataria, J.; Devi, P.; Rani, P. Importance of structures and interactions in ionic liquid-nanomaterial composite systems as a novel approach for their utilization in safe lithium metal batteries: A review. *J. Mol. Liq.* **2021**, *339*, 116736. [CrossRef]

20. Smith, E.L.; Abbott, A.P.; Ryder, K.S. Deep Eutectic Solvents (DESs) and Their Applications. *Chem. Rev.* **2014**, *114*, 11060–11082. [CrossRef]

21. Zaib, Q.; Adeyemi, I.; Warsinger, D.M.; AlNashef, I.M. Deep Eutectic Solvent Assisted Dispersion of Carbon Nanotubes in Water. *Front. Chem.* **2020**, *8*, 808. [CrossRef]

22. Izutsu, K. Fundamentals of Chemistry in Nonaqueous Solutions: Electrochemical Aspects. In *Electrochemistry in Nonaqueous Solutions*; Wiley: New York, NY, USA, 2009; ISBN 978-3-527-62916-9.

23. Koczkur, K.M.; Mourdikoudis, S.; Polavarapu, L.; Skrabalak, S.E. Polyvinylpyrrolidone (PVP) in nanoparticle synthesis. *Dalt. Trans.* **2015**, *44*, 17883–17905. [CrossRef] [PubMed]

24. Brandão, A.T.S.C.; Rosoiu, S.; Costa, R.; Lazar, O.A.; Silva, A.F.; Anicai, L.; Pereira, C.M.; Enachescu, M. Characterization and electrochemical studies of MWCNTs decorated with Ag nanoparticles through pulse reversed current electrodeposition using a deep eutectic solvent for energy storage applications. *J. Mater. Res. Technol.* **2021**, *15*, 342–359. [CrossRef]

25. Freire, M.G.; Teles, A.R.R.; Rocha, M.A.A.; Schröder, B.; Neves, C.M.S.S.; Carvalho, P.J.; Evtuguin, D.V.; Santos, L.M.N.B.F.; Coutinho, J.A.P. Thermophysical characterization of ionic liquids able to dissolve biomass. *J. Chem. Eng. Data* **2011**, *56*, 4813–4822. [CrossRef]

26. Ibrahim, T.H.; Sabri, M.A.; Jabbar, N.A.; Nancarrow, P.; Mjalli, F.S.; AlNashef, I. Thermal Conductivities of Choline Chloride-Based Deep Eutectic Solvents and Their Mixtures with Water: Measurement and Estimation. *Molecules* **2020**, *25*, 3816. [CrossRef]

27. Crespo, E.A.; Costa, J.M.L.; Palma, A.M.; Soares, B.; Martín, M.C.; Segovia, J.J.; Carvalho, P.J.; Coutinho, J.A.P. Thermodynamic characterization of deep eutectic solvents at high pressures. *Fluid Phase Equilib.* **2019**, *500*, 112249. [CrossRef]

28. Xu, X.; Range, J.; Gygli, G.; Pleiss, J. Analysis of Thermophysical Properties of Deep Eutectic Solvents by Data Integration. *J. Chem. Eng. Data* **2020**, *65*, 1172–1179. [CrossRef]

29. Neves, C.M.S.S.; Batista, M.L.S.; Cláudio, A.F.M.; Santos, L.M.N.B.F.; Marrucho, I.M.; Freire, M.G.; Coutinho, J.A.P. Thermophysical properties and water saturation of [PF6]-based ionic liquids. *J. Chem. Eng. Data* **2010**, *55*, 5065–5073. [CrossRef]

30. Tariq, M.; Forte, P.A.S.; Gomes, M.F.C.; Lopes, J.N.C.; Rebelo, L.P.N. Densities and refractive indices of imidazolium- and phosphonium-based ionic liquids: Effect of temperature, alkyl chain length, and anion. *J. Chem. Thermodyn.* **2009**, *41*, 790–798. [CrossRef]

31. Almeida, H.F.D.; Passos, H.; Lopes-Da-Silva, J.A.; Fernandes, A.M.; Freire, M.G.; Coutinho, J.A.P. Thermophysical properties of five acetate-based ionic liquids. *J. Chem. Eng. Data* **2012**, *57*, 3005–3013. [CrossRef]

32. Xu, A.; Zhang, Y.; Lu, W.; Yao, K.; Xu, H. Effect of alkyl chain length in anion on dissolution of cellulose in 1-butyl-3-methylimidazolium carboxylate ionic liquids. *J. Mol. Liq.* **2014**, *197*, 211–214. [CrossRef]

33. Coutinho, J.A.P.; Carvalho, P.J.; Oliveira, N.M.C. Predictive methods for the estimation of thermophysical properties of ionic liquids. *RSC Adv.* **2012**, *2*, 7322–7346. [CrossRef]

34. Fukushima, T.; Kosaka, A.; Ishimura, Y.; Yamamoto, T.; Takigawa, T.; Ishii, N.; Aida, T. Molecular ordering of organic molten salts triggered by single-walled carbon nanotubes. *Science* **2003**, *300*, 2072–2074. [CrossRef] [PubMed]

35. Hameed, N.; Church, J.S.; Salim, N.V.; Hanley, T.L.; Amini, A.; Fox, B.L. Dispersing single-walled carbon nanotubes in ionic liquids: A quantitative analysis. *RSC Adv.* **2013**, *3*, 20034–20039. [CrossRef]

36. Wang, J.; Chu, H.; Li, Y. Why Single-Walled Carbon Nanotubes Can Be Dispersed in Imidazolium-Based Ionic Liquids. *ACS Nano* **2008**, *2*, 2540–2546. [CrossRef] [PubMed]

37. Polo-Luque, M.L.; Simonet, B.M.; Valcárcel, M. Functionalization and dispersion of carbon nanotubes in ionic liquids. *TrAC Trends Anal. Chem.* **2013**, *47*, 99–110. [CrossRef]

38. Chen, Y.Y.; Walvekar, R.; Khalid, M.; Shahbaz, K.; Gupta, T.C.S.M. Stability and thermophysical studies on deep eutectic solvent based carbon nanotube nanofluid. *Mater. Res. Express* **2017**, *4*, 075028. [CrossRef]

39. Chen, L.; Deng, J.; Song, Y.; Hong, S.; Lian, H. Highly Stable Dispersion of Carbon Nanotubes in Deep Eutectic Solvent for the Preparation of CNT-Embedded Carbon Xerogels for Supercapacitors. *ChemElectroChem* **2019**, *6*, 5750–5758. [CrossRef]

40. Walvekar, R.; Singh, A.; Khalid, M.; Gupta, T.; Yin, W.W. Thermophysical properties of deep eutectic solvent-carbon nanotubes (DES-CNT) based nanolubricant. *J. Therm. Eng.* **2020**, *6*, 53–64. [CrossRef]

41. Vakili-Nezhaad, G.; Dorany, A. Effect of single-walled carbon nanotube on the viscosity of lubricants. *Energy Procedia* **2012**, *14*, 512–517. [CrossRef]

42. Vakili-Nezhaad, G.R.; Dorany, A. Investigation of the effect of multiwalled carbon nanotubes on the viscosity index of lube oil cuts. *Chem. Eng. Commun.* **2009**, *196*, 997–1007. [CrossRef]

43. Ma, P.C.; Siddiqui, N.A.; Marom, G.; Kim, J.K. Dispersion and functionalization of carbon nanotubes for polymer-based nanocomposites: A review. *Compos. Part A Appl. Sci. Manuf.* **2010**, *41*, 1345–1367. [CrossRef]

44. Luo, R.; Li, Q.; Du, B.; Zhou, S.; Chen, Y. Preparation and Characterization of Solid Electrolyte Doped with Carbon Nanotubes and its Preliminary Application in $NO_2$ Gas Sensors. *Front. Mater.* **2019**, *6*, 113. [CrossRef]

45. Wang, Y.C.; Huang, K.C.; Dong, R.X.; Te Liu, C.; Wang, C.C.; Ho, K.C.; Lin, J.J. Polymer-dispersed MWCNT gel electrolytes for high performance of dye-sensitized solar cells. *J. Mater. Chem.* **2012**, *22*, 6982–6989. [CrossRef]

46. Tamate, R.; Saruwatari, A.; Nakanishi, A.; Matsumae, Y.; Ueno, K.; Dokko, K.; Watanabe, M. Excellent dispersibility of single-walled carbon nanotubes in highly concentrated electrolytes and application to gel electrode for Li-S batteries. *Electrochem. Commun.* **2019**, *109*, 106598. [CrossRef]

47. Azizighannad, S.; Wang, Z.; Siddiqui, Z.; Kumar, V.; Mitra, S. Nano carbon doped polyacrylamide gel electrolytes for high performance supercapacitors. *Molecules* **2021**, *26*, 2631. [CrossRef] [PubMed]

48. Jiang, K.; Gerhardt, R.A. Fabrication and Supercapacitor Applications of Multiwall Carbon Nanotube Thin Films. *C* **2021**, *7*, 70. [CrossRef]

49. Deshiikan, S.R.; Papadopoulos, K.D. Modified Booth equation for the calculation of zeta potential. *Colloid Polym. Sci.* **1998**, *276*, 117–124. [CrossRef]

50. David, R. Lide Concentrative properties of aqueous solutions: Density, refractive index, freezing point depression, and viscosity. In *CRC Handbook of Chemistry and Physics: A Ready-Reference Book of Chemical and Physical Data*; CRC Press: Boca Raton, FL, USA, 1997; ISBN B008VROK8M.

51. Daerr, A.; Mogne, A. Pendent_Drop: An ImageJ Plugin to Measure the Surface Tension from an Image of a Pendent Drop. *J. Open Res. Softw.* **2016**, *4*, 2–6.

52. Sabri, F.N.A.M.; Zakaria, M.R.; Akil, H.M. Dispersion and stability of multiwalled carbon nanotubes (MWCNTs) in different solvents. *AIP Conf. Proc.* **2020**, *2267*, 20043.

53. Hanzel, O.; Sedláček, J.; Šajgalík, P. New approach for distribution of carbon nanotubes in alumina matrix. *J. Eur. Ceram. Soc.* **2014**, *34*, 1845–1851. [CrossRef]

54. Mjalli, F.S.; Naser, J.; Jibril, B.; Alizadeh, V.; Gano, Z. Tetrabutylammonium Chloride Based Ionic Liquid Analogues and Their Physical Properties. *J. Chem. Eng. Data* **2014**, *59*, 2242–2251. [CrossRef]

55. Nowosielski, B.; Jamrógiewicz, M.; Łuczak, J.; Śmiechowski, M.; Warmińska, D. Experimental and predicted physicochemical properties of monopropanolamine-based deep eutectic solvents. *J. Mol. Liq.* **2020**, *309*, 113110. [CrossRef]

56. Tang, B.; Row, K.H. Recent developments in deep eutectic solvents in chemical sciences. *Monatshefte Chem. Chem. Mon.* **2013**, *144*, 1427–1454. [CrossRef]

57. Wang, Y.; Ma, C.; Liu, C.; Lu, X.; Feng, X.; Ji, X. Thermodynamic Study of Choline Chloride-Based Deep Eutectic Solvents with Water and Methanol. *J. Chem. Eng. Data* **2020**, *65*, 2446–2457. [CrossRef]

58. Rumble, J.R. (Ed.) *CRC Handbook of Chemistry and Physics*, 102nd ed.; CRC Press: Boca Raton, FL, USA; Taylor & Francis: Abingdon, UK, 2004.

59. Al-Murshedi, A.Y.M.; Alesary, H.F.; Al-Hadrawi, R. Thermophysical properties in deep eutectic solvents with/without water. *J. Phys. Conf. Ser.* **2019**, *1294*, 052041. [CrossRef]

60. AlOmar, M.K.; Hayyan, M.; Alsaadi, M.A.; Akib, S.; Hayyan, A.; Hashim, M.A. Glycerol-based deep eutectic solvents: Physical properties. *J. Mol. Liq.* **2016**, *215*, 98–103. [CrossRef]

61. Wang, F.; Wang, F.; Fan, X.; Lian, Z. Experimental study on an inverter heat pump with HFC125 operating near the refrigerant critical point. *Appl. Therm. Eng.* **2012**, *39*, 1–7. [CrossRef]

62. Wang, B.; Wang, X.; Lou, W.; Hao, J. Rheological and Tribological Properties of Ionic Liquid-Based Nanofluids Containing Functionalized Multi-Walled Carbon Nanotubes. *J. Phys. Chem. C* **2010**, *114*, 8749–8754. [CrossRef]

63. Alizadeh, J.; Keshavarz Moraveji, M. An experimental evaluation on thermophysical properties of functionalized graphene nanoplatelets ionanofluids. *Int. Commun. Heat Mass Transf.* **2018**, *98*, 31–40. [CrossRef]

64. Awais, M.; Ullah, N.; Ahmad, J.; Sikandar, F.; Ehsan, M.M.; Salehin, S.; Bhuiyan, A.A. Heat transfer and pressure drop performance of Nanofluid: A state-of- the-art review. *Int. J. Thermofluids* **2021**, *9*, 100065. [CrossRef]

65. Protsenko, V.S.; Kityk, A.A.; Shaiderov, D.A.; Danilov, F.I. Effect of water content on physicochemical properties and electrochemical behavior of ionic liquids containing choline chloride, ethylene glycol and hydrated nickel chloride. *J. Mol. Liq.* **2015**, *212*, 716–722. [CrossRef]

66. Ghosh, S.; Ryder, K.; Roy, S. Electrochemical and transport properties of ethaline containing copper and tin chloride. *Trans. IMF* **2014**, *92*, 41–46. [CrossRef]

67. Chen, Y.; Chen, W.; Fu, L.; Yang, Y.; Wang, Y.; Hu, X.; Wang, F.; Mu, T. Surface Tension of 50 Deep Eutectic Solvents: Effect of Hydrogen-Bonding Donors, Hydrogen-Bonding Acceptors, Other Solvents, and Temperature. *Ind. Eng. Chem. Res.* **2019**, *58*, 12741–12750. [CrossRef]

68. Abbott, A.P.; Boothby, D.; Capper, G.; Davies, D.L.; Rasheed, R.K. Deep Eutectic Solvents formed between choline chloride and carboxylic acids: Versatile alternatives to ionic liquids. *J. Am. Chem. Soc.* **2004**, *126*, 9142–9147. [CrossRef] [PubMed]

69. Sa, V.; Kornev, K.G. Analysis of Stability of Nanotube Dispersions Using Surface Tension Isotherms. *Langmuir* **2011**, *27*, 13451–13460. [CrossRef]

70. Abbott, A.P.; Capper, G.; Gray, S. Design of Improved Deep Eutectic Solvents Using Hole Theory. *ChemPhysChem* **2006**, *7*, 803–806. [CrossRef]

71. Abbott, A.P. Application of Hole Theory to the Viscosity of Ionic and Molecular Liquids. *ChemPhysChem* **2004**, *5*, 1242–1246. [CrossRef]

72. Fürth, R. On the theory of the liquid state: I. The statistical treatment of the thermodynamics of liquids by the theory of holes. *Math. Proc. Cambridge Philos. Soc.* **1941**, *37*, 252–275. [CrossRef]

73. Bockris, J.O.; Richards, N.E. The Compressibilities, Free Volumes and Equation of State for Molten Electrolytes: Some Alkali Halides and Nitrates. *Proc. R. Soc. Lond. A. Math. Phys. Sci.* **1957**, *241*, 44–66.

74. Abbott, A.P.; Barron, J.C.; Ryder, K.S.; Wilson, D. Eutectic-based ionic liquids with metal-containing anions and cations. *Chem. A Eur. J.* **2007**, *13*, 6495–6501. [CrossRef]

75. Gabriele, F.; Chiarini, M.; Germani, R.; Tiecco, M.; Spreti, N. Effect of water addition on choline chloride/glycol deep eutectic solvents: Characterization of their structural and physicochemical properties. *J. Mol. Liq.* **2019**, *291*, 111301. [CrossRef]

76. Abbott, A.P.; Harris, R.C.; Ryder, K.S.; D'Agostino, C.; Gladden, L.F.; Mantle, M.D. Glycerol eutectics as sustainable solvent systems. *Green Chem.* **2011**, *13*, 82–90. [CrossRef]

77. Mehrali, M.; Sadeghinezhad, E.; Rashidi, M.M.; Akhiani, A.R.; Tahan Latibari, S.; Mehrali, M.; Metselaar, H.S.C. Experimental and numerical investigation of the effective electrical conductivity of nitrogen-doped graphene nanofluids. *J. Nanoparticle Res.* **2015**, *17*, 267. [CrossRef]

78. Baby, T.T.; Ramaprabhu, S. Investigation of thermal and electrical conductivity of graphene based nanofluids. *J. Appl. Phys.* **2010**, *108*, 124308. [CrossRef]

79. Nabati Shoghl, S.; Jamali, J.; Keshavarz Moraveji, M. Electrical conductivity, viscosity, and density of different nanofluids: An experimental study. *Exp. Therm. Fluid Sci.* **2016**, *74*, 339–346. [CrossRef]

80. Kausar, A.; Siddiq, M. Carbon nanotubes/silver nanoparticles/poly(azo-thiourea) hybrids: Morphological, tensile and conductivity profile. *J. Compos. Mater.* **2014**, *48*, 3271–3280. [CrossRef]

81. Shaikh, M.S.; Shariff, A.M.; Bustam, M.A.; Murshid, G. Physicochemical Properties of Aqueous Solutions of Sodium l-Prolinate as an Absorbent for $CO_2$ Removal. *J. Chem. Eng. Data* **2014**, *59*, 362–368. [CrossRef]

82. Navarro, S.S.; Leron, R.B.; Soriano, A.N.; Li, M.-H. Thermophysical property characterization of aqueous amino acid salt solution containing serine. *J. Chem. Thermodyn.* **2014**, *78*, 23–31. [CrossRef]

83. Murshid, G.; Shariff, A.M.; Keong, L.K.; Bustam, M.A. Physical Properties of Aqueous Solutions of Piperazine and (2-Amino-2-methyl-1-propanol + Piperazine) from (298.15 to 333.15) K. *J. Chem. Eng. Data* **2011**, *56*, 2660–2663. [CrossRef]

84. Leron, R.B.; Soriano, A.N.; Li, M.-H. Densities and refractive indices of the deep eutectic solvents (choline chloride+ethylene glycol or glycerol) and their aqueous mixtures at the temperature ranging from 298.15 to 333.15K. *J. Taiwan Inst. Chem. Eng.* **2012**, *43*, 551–557. [CrossRef]

85. Shahriari, E.; Moradi, M.; Varnamkhasti, M.G. Investigation of nonlinear optical properties of Ag nanoparticles. *Int. J. Opt. Photonics* **2015**, *9*, 107–114.